# Design optimisation for a hybrid renewable microgrid

## Application to the case of Faial Island, Azores Archipelago

**Marco Barbaro**

Thesis to obtain the Master of Science Degree in

**Energy Engineering and Management**

Supervisor: Prof. Rui Manuel Gameiro de Castro

**Examination Committee**

Chairperson: Prof. Jorge de Saldanha Gonçalves Matos

Supervisor: Prof. Rui Manuel Gameiro de Castro

Member of the Committee: Prof. Carlos Augusto Santos Silva

**October 2018**

# ACKNOWLEDGEMENTS

This thesis has been a long, difficult work not only for its technical aspects but also from a personal point of view. Many people supported me during this journey, and without their help and encouragement this work would probably look different from how it is.

I want to thank my program coordinator Duarte de Mesquita e Sousa and my supervisor Rui Castro for their encouragement not to give up when things seemed too complicated, and my friends Luigi, Carmine and Bodil for their constant support and advice.

Without the help of António Setas Lopes and the patience and collaboration of engineer David Estrela from EDA, it would have been very difficult to obtain accurate and up-to-date data and information to use in the case study, so a very big *thank you* goes to them.

I need to express my gratitude to my parents and to Chiara for all the encouragement, the trust, the support, the love and the motivation they gave me from the very beginning of this university journey.

Finally, I dedicate a great hug to the InnoEnergy and SELECT family, without whom I would not be here writing this today.

# ABSTRACT

The integration of intermittent renewable energy sources represents a great challenge for any energy system. In particular, islanded microgrids with a high penetration of renewables experience a strong need for technologies that allow to match demand and production at any moment, which are still largely represented by fossil fuel generators.

This MSc thesis work aims at proposing an optimised design for the energy system of Faial, an island in the Açores archipelago, featuring the highest possible renewable energy penetration which can be obtained respecting the technological and financial feasibility constraints. Faial has a significant potential for resources such as solar, wind and micro-hydro, which are already partially exploited, although 88.8% of the yearly energy production is currently ensured by diesel and fuel oil generators.

To the purpose of investigating a possible increase of the renewable penetration in the island, a MatLab model has been developed, using weather and electric demand measured data to combine and size optimally the components of a hybrid energy system featuring wind, photovoltaic, geothermal and diesel generators, as well as battery energy storage systems (BESS). The model can be varied in its contraints to fit at best the multi-objective nature of the problem, where the conflicting objectives are the Net Present Value (NPV) of the system design, its Renewable Energy Fraction (REF) and the Energy Index of Reliability (EIR), defined as the percentage of demanded energy that is matched by the generators.

Once a set of possible optimal design has ben determined, a system design featuring 5504 kW of geothermal installed power and 6208 kWh of BESS capacity, together with the already present thermal generators and 4250 kW of wind turbines, has been analysed more in detail. Such system design, totalising an initial investment of 28.85 M€, has a NPV of only 43'000€ when compared to the current system configuration, which anyway can rise to roughly 6 M€ with an adjustment of the electricity retail price of around 10 €/MWh. The adopted UC model has shown that some of the thermal generators on the island remain unused, apart from during maintenance ad servicing of other gensets. Monte Carlo simulations with synthetic time series have been performed to investigate the impact on the project of the variability in wind speed and in energy demand, highlighting the robustness of the selected design.

**Keywords:** hybrid renewable microgrid; optimisation; Monte Carlo simulations; stochastic processes; synthetic time series; Azores.

# RESUMO

A integração de fontes de energia renováveis intermitentes representa um grande desafio para qualquer sistema energético, em particular, nas microrredes em ilhas, onde as tecnologias que permitem combinar a procura e a produção a qualquer momento ainda são asseguradas por geradores de combustíveis fósseis.

Este trabalho visa propor um sistema de produção elétrica otimizado para abastecimento da ilha do Faial, no arquipélago dos Açores. O projeto propõe a configuração do sistema eletroprodutor que visa obter a mais alta penetração possível de energia renovável, respeitando as restrições tecnológicas e de viabilidade financeira. O Faial tem um potencial significativo para recursos como solar, eólica e micro-hídrica, que já são parcialmente explorados, embora quase 90% da produção anual de eletricidade seja atualmente assegurada por geradores a diesel.

Com o objetivo de investigar um possível aumento da penetração de fontes renováveis na ilha, desenvolveu-se um modelo específico aplicado ao sistema elétrico do Faial. Usaram-se dados meteorológicos medidos, bem como dados do consumo de energia elétrica para combinar e dimensionar os componentes de um sistema híbrido de energia eólica, fotovoltaica, geotérmica e geradores diesel, bem como sistemas de armazenamento de energia por bateria (BESS). O modelo é suficientemente flexível para melhor se adequar à natureza multi-objetivo do problema, onde os objetivos conflituantes são o Valor Atual Líquido (VAL) do projeto, a Fração de Energia Renovável e o Índice de Confiabilidade de Energia.

Uma vez determinado um conjunto de possíveis configurações ótimas, a configuração correspondente a 5504 kW de potência geotérmica instalada e 6208 kWh de capacidade de baterias, juntamente com os já existentes geradores térmicos e 4250 kW de turbinas eólicas, foi analisada em mais detalhes. Tal desenho do sistema, totalizando um investimento inicial de 28,85 M€, tem um VAL de apenas 43 000 € quando comparado com a configuração atual do sistema; no entanto, o VAL pode subir para cerca de 6 M€ com um ajuste no preço de venda a retalho de cerca de 10 €/MWh. O modelo proposto, que inclui um módulo de Unit Commitment, mostrou que alguns dos geradores térmicos da ilha permanecem ociosos, exceto durante a manutenção de outros grupos geradores. Efetuou-se ainda uma análise de sensibilidade usando Simulações de Monte Carlo, com séries temporais sintéticas, para investigar o impacto da variação da velocidade do vento e do consumo elétrico.

**Palavras-chave:** microrredes; energia rénovável; otimização; simulações de Monte Carlo; processos estocásticos; séries temporais sintéticas; Açores.

# List of Abbreviations and Symbols

**ABBREVIATIONS**

| | | | |
|---|---|---|---|
| **BESS** | Battery Energy Storage System | **HFO** | Heavy Fuel Oil |
| **CDF** | Cumulative probability density function | **HV/MV/LV** | High / Medium / Low Voltage |
| **CF** | Cash Flows | **IRR** | Internal Rate of Return [%] |
| **CRF** | Capital Recovery Factor [ - ] | **IST** | Instituto Superior Técnico |
| **DNI** | Direct Normal Irradiation [W/m$^2$] | **MIRR** | Modified Internal Rate of Return [%] |
| **DOD** | Battery Depth of Discharge | **NOPAT** | Net Operating Profit After Taxes [€] |
| **EBIT** | Earning Before Interests and Taxes [€] | **NPV** | Net Present Value [€] |
| **EBITDA** | Earning Before Interests, Taxes, Depreciation and Amortisation [€] | **PDF** | Probability Density Function |
| **EDA** | Electricidade dos Açores | **PF** | Power factor [kW / kVAR] |
| **EENS** | Expected Energy Not Served | **REF** | Renewable Energy Fraction [%] |
| **EIR** | Energy Index of Reliability [%] | **RES** | Renewable Energy Sources |
| **FFCF** | Free Cash Flows to Firm [€/y] | **SR** | Spinning Reserve |
| **GHI** | Global Horizontal Irradiation [W/m$^2$] | **TMY** | Typical Meteorological Year |
| **HAWS** | Hourly Average Wind Speed [m/s] | **WACC** | Weighted Average Cost of Capital [%] |
| **HES** | Hybrid Energy System | | |

**SYMBOLS**

| | | | |
|---|---|---|---|
| $A_i$ | Anisotropy index [ - ] | $I_{d,iso}$ | Isotropic diffuse irradiance [W/m$^2$] |
| $\beta$ | Tilt angle of PV panels [ ° ] | $I_{d,cs}$ | Circumsolar diffuse irradiance [W/m$^2$] |
| $C_B$ | Nominal capacity of BESS [kWh] | $I_{d,hz}$ | Horizon-brightening diffuse irradiance [W/m$^2$] |
| $C_{max}^{therm}$ | Nominal power of thermal generators [kW] | $I_r$ | Ground-reflected irradiance [W/m$^2$] |
| $C_{min}^{therm}$ | Minimum amount of energy production allowed in a time step bythermal generators [kWh] | $int$ | Interests [€] |
| $Cost_{t,i}$ | operating cost of generator $i$ at time $t$ [€/h] | $LB/UB$ | Lower and Upper bounds of the decision variable vector $x$ |
| $E_{disch}^{BESS}$ | Energy discharged by BESS [kWh] | $P_{MWt,i}^{therm}$ | Power output of generator $i$ at time $t$ [MW] |
| $E_{into}^{BESS}$ | Theoretical energy in the BESS at the end of a time step, ignoring the lower and upper charge limits [kWh] | $P_t^{wind}$ | Power output of all wind turbines at time $t$ [kW] |
| $E_{to}^{BESS}$ | Energy sent or requested from BESS [kWh] | $r$ | Interest rate on debt [%] |
| $E_{curt}$ | Energy curtailed [kWh] | $rv$ | Residual value [%] |
| $E_{load}$ | Energy demand in a time period [kWh] | $\rho_g$ | ground reflectance |
| $E_{RES}$ | Energy produced by RES [kWh] | $SoC_{bop}$ | State of Charge of BESS at beginning of period [ - ] |
| $E_{SR}$ | Required spinning reserve energy to be produced at a certain time step [kWh] | $SoC_{eop}$ | State of Charge of BESS at end of period [ - ] |
| $E_{thermal}$ | Energy production from thermal generators additional to SR to match the load [kWh] | $SoC_{min}$ | Minimum State of Charge allowed by BESS [ - ] |
| $\eta_{BESS}$ | Efficiency of charge and discharge of the BESS [%] | $StUp_i$ | Startup cost of generator i [€] |
| $I_T$ | Total irradiance [W/m$^2$] | $R_b$ | Ratio of diffuse radiation on the tilted surface to that on the horizontal plane |
| $I_b$ | Beam irradiance [W/m$^2$] | $x$ | Vector of the decision variables |

# TABLE OF CONTENTS

Acknowledgements ..... 3

Abstract ..... 5

Resumo ..... 6

List of Abbreviations and Symbols ..... 8

Table of contents ..... 10

List of tables ..... 12

List of figures ..... 13

1. Introduction ..... 14

   1.1. Objectives ..... 15

   1.2. Structure of the thesis ..... 15

2. Literature review ..... 16

   2.1. The microgrid model ..... 16

   2.2. Optimisation algorithms ..... 17

   2.3. Azores' energy challenges ..... 18

3. Methodology ..... 20

   3.1. Simulation model ..... 20

   3.2. Optimisation model ..... 23

   3.3. Unit Commitment and Economic Dispatch ..... 25

   3.4. Financial model ..... 26

4. The Faial Case Study ..... 28

   4.1. Energy system in Faial ..... 29

   4.2. Trends in electric production and consumption ..... 31

5. Input data and synthetic time series generation ..... 33

   5.1. Electricity demand ..... 33

   5.2. Wind speed ..... 34

   5.3. Solar irradiation ..... 37

   5.4. Geothermal and Energy Storage ..... 39

   5.5. Thermal generators ..... 39

   5.6. Economic input data ..... 43

6. Results ..... 46
6.1. Base cases ..... 46
6.2. The scenarios ..... 47
6.3. Sensitivity analysis and Monte Carlo simulations ..... 51
7. Conclusions ..... 56
References ..... 58
Annex A – Optimisation results in detail ..... 64

# LIST OF TABLES

Table 1 – Electricity monthly production in Faial in 2017 [39] .......... 30

Table 2 – Summary of fuel generators in Faial .......... 31

Table 3 – Summary of chosen PV panel's characteristics .......... 37

Table 4 – Air temperatures used in the model, in an hour/month axes system .......... 38

Table 5 – Summary of the hourly cost parametres for the thermal generators in Faial .......... 40

Table 6 – Evolution of interest rates for EDA in years 2008 - 2016 .......... 43

Table 7 – Summary of Capex and Opex costs for the technologies of the decision variables .......... 44

Table 8 – Simulation results. Top line is with geothermal, while bottom line is without geothermal ..... 49

Table 9 – Simulation results with limitation of PV capacity at 1.5 MW .......... 50

Table 10 – Installed capacity in the design chosen for sensitivity analysis .......... 51

Table 11 – Optimisation results in detail, with NPV maximised in comparison with respective base case .......... 64

Table 12 – Optimisation results with 1.5 MW limitation on PV .......... 65

# List of figures

Figure 1 – Logical scheme of the system ........ 20

Figure 2 – Power curve of Vestas V52/850 [31] ........ 21

Figure 4 – Logical scheme of UC model ........ 25

Figure 5 – Electricity production mix in the Azores in 2016 [34] [35] ........ 28

Figure 6 – Breakdown of electricity consumption in December 2017 in Faial [38] ........ 29

Figure 7 – Map of electric grid in Faial [34] ........ 30

Figure 8 – Total energy production in Faial in years 2009 – 2017 [39] ........ 32

Figure 9 – Wind and hydro electricity generation in years 2009 - 2017 [39] ........ 32

Figure 10 – Sample of load curves measured by EDA in 2017 ........ 33

Figure 11 – Plot of a hourly load curve obtained with the stochastic approach ........ 34

Figure 12 – Histogram of estimated wind speeds for year 2017, at height of 100 metres ........ 35

Figure 13 – Relative probability for the absolute value of HAWS variation over consecutive hours ........ 36

Figure 14 – Representation of some of the randomly generated yearly wind speeds (in blue) normalised histograms against the sample year (in orange) ........ 37

Figure 15 – Variation of parametres for quadratic programming ED with generator size ........ 41

Figure 16 – Operating cost in €/h as a function of the output power of each generator ........ 41

Figure 17 – Variation of startup cost with generator rated power ........ 41

Figure 18 – Cost projections for PV panels ........ 44

Figure 19 – Benchmark NPV of the three base cases, for calculation of compared NPV ........ 46

Figure 20 – NPV of the optimal designs, with and without geothermal, varying REF and carbon tax.. 48

Figure 21 – NPV of the optimal designs with PV limitation at 1.5 MW ........ 48

Figure 22 – Detail of the optimisation results with limit on PV and carbon tax 6 €/ton$_{CO2}$ ........ 51

Figure 23 – Breakdown of energy production from the selected design ........ 52

Figure 24 – Hours of usage of thermal engines in the chosen design, and breakdown of corresponding energy production ........ 53

Figure 25 – Comparison of the results of the optimisation with one of the optimal designs from HOMER ........ 53

Figure 26 – Sensitivity analysis on electricity retail price ........ 54

Figure 27 – Sensitivity analysis on interest rate over debt with base electricity price ........ 54

Figure 28 – Monte Carlo simulations of project NPV depending on wind conditions, with electricity retail price of 162.85 €/MWh and 175 €/MWh ........ 55

Figure 29 – Monte Carlo simulation of project NPV with load curve uncertainty ........ 55

# 1. INTRODUCTION

Energy transition is one of the greatest technological challenge of the XXI century. The energy generation scene is becoming more and more dominated by renewables: even in IEA World Energy Outlook's *current policies scenario*, the least ambitious scenario in terms of decarbonisation, renewable energy sources (RES) represent 28.8% of world's electricity production [1]. The increase in renewable share is leading in a shift in the production paradigm from centralised to distributed generation, radically transforming the traditional notion of energy system. Anyway, due to the intermittant nature of the resources exploited by RES, the road to clean energy transition is not without challenges, especially in smaller energy systems such as microgrids, which are more sensitive to power oscillations in the network.

Microgrids are small-scale power networks independent from the main large energy transmission systems, sometimes interconnectable, and sometimes completely separated because of geographical constraints. The concept of microgrid is becoming more and more widespread, not only in small islands or remote communities, but also in modular configurations inside large grids, allowing different districts and facilities to be independent from each other in case of need and to work independently with a higher resilience in the event of network outages. When operating in island mode, microgrids are characterised by high fuel costs, as the need for network stability limits the penetration of RES [2]. On the other hand, RES provide new solutions against the progressive inefficiency and high expenses of conventional energy systems in island regions.

Just in Europe there are about 300 islands (6% of the Union Territory) with 14 million inhabitants, more than the whole population of some member states such as Portugal [2]. In many cases, such islands are not connected to the mainland's energy network, and rely on their own microgrid, offering a good terrain for experimenting new technologies and concepts. The economy of most islands relies on tourism, and many of them are part of natural reserves as well, hence the need for cleaner solutions to fulfill their energy needs in respect of the environment and on the public health.

This thesis proposes a modeling and optimisation tool to determine the optimal configuration of the energy system of an island-mode microgrid and the highest RES penetration that can be achieved, keeping into account not only the constraints related to weather conditions and technological limits but also those derivated from the economical and financial viability of a project. The model has been fit and tested with the case-study of Faial island, in the Portuguese archipelago of the Azores.

EDA, the utility company in the Azores, has a strategic plan which involves investing 130 M€ in years 2018-2022 [3] only for renewables and storage systems, such as new pumped hydro systems in São Miguel and Terceira, an innovative hybrid system with battery storage in Graciosa, and a 600 kW photovoltaic plant in Santa Maria. This figure is very significant, considering that the EBITDA of EDA in 2016 was around 50 M€; in addition, the company is supported by EU funds with a very low interest rate, as more extensively presented in section 5.6. This thesis focuses on analysing the potential role of Faial in this framework, studying the impact and the challenges of developing a project for a hybrid renewable microgrid.

## 1.1. OBJECTIVES

The scope of this work is to formulate a general model to investigate the possible increase of the renewable penetration in an island-mode microgrid, with a specific focus on the island of Faial, Azores. To this purpose, the following objectives have been defined:

- Develop a simulation model which uses weather and electric demand measured data to evaluate the electricity generation of a hybrid renewable islanded energy system at hourly time step by using a Unit Commitment (UC) algorithm, and to estimate the Net Present Value of the system configuration over 20 years
- Develop an optimisation model that iterates on the aforementioned simulation model, allowing to combine and size optimally the components of a hybrid energy system featuring wind, photovoltaic, geothermal and diesel generators, as well as battery energy storage systems (BESS). Such model should be flexible and allow the user to vary its constraints, in order to explore the multi-objective nature of the optimisation problem.
- Apply the optimisation model to the case-study of Faial island in the Azores, to validate it and to evaluate the renewable potential that can be realistically installed in the island in the respect of the technological and economical constraints.
- Identify and develop a methodology to elaborate the measured wind and electricity demand data in Faial for generating synthetic time series, and use such time series to evaluate the variations in the outputs of the model by the use of Monte Carlo simulations.
- Perform a sensitivity analysis of the optimal solution found by the model, by varying the values of the input parametres and evaluating their impact on the energetic and economic outcomes.

## 1.2. STRUCTURE OF THE THESIS

The present work is divided into seven main chapters, in which the content is distributed as follows:

- Chapter 1 offers an introduction to this work, outlines its objectives and schematise the structure of the thesis.
- Chapter 2 encloses a literature review on the topics of microgrids, optimisation algorithms, and the energy challenges in the Azores.
- Chapter 3 describes the simulation and optimisation model developed in this work, with a particular focus on the UC model and on the financial parametres which have been used.
- Chapter 4 is structured as an introduction to the Faial case study, describing the current energy situation in the island
- Chapter 5 presents in detail the input data and the methodology used for the elaboration of synthetic time series to use for Monte Carlo simulations once the optimal design of the system has been identified.
- Chapter 6 presents the results of the optimisation, describes the optimal system configuration that has been chosen, and reports the sensitivity analyses which have been performed on it.
- Chapter 7 outlines the conclusions taken from this thesis work.

# 2. Literature review

In the past years, the scientific community has dedicated a great amount of effort and work to the topic of microgrid modeling and optimisation, investigating also the future potential and applications of this energy system paradigm. On the more mathematical side, new optimisation algorithms have been developed and studied, in an increasing scale of sophistication, spacing from exact algorithms derived from linear programming, to more efficient but less precise heuristic methods such as genetic algorithms or particle-swarm optimisations.

As well as that, several studies have targeted the region of the Açores as a case study, touching interests of both the industry and research sides, due to the technological challenges and abundance of energy resources of the archipelago.

This section aims at summarising the highlights of the work that has been performed in other studies on these three macro-subjects that are the backbone of this thesis: microgrids, optimisation models and energy trends in the Açores.

## 2.1. The microgrid model

Renewable-based microgrids are becoming more and more common, especially in developing countries where electrification levels are low and several areas are not reached by the national grid. Renewables allow a distributed generation in the same area where the energy is needed. The potential of microgrids applied to rural electrification is enormous, especially thinking of its socio-economic impact, as estimated for example in [4] and [5].

[6] illustrates how the microgrid concept can be applied in a modular way to allow large scale deployment of distributed RES in conventional grids. The paper analyses the most recend developments in microgrids and in system components, with a particular focus on control systems and power electronics. Throughout several examples of projects in world, highlighting the work which is currently being performed by industry and research, the authors support the idea that the paradigm of microgrids will have a fundamental role in the future development of energy systems with high renewable penetration.

Anyway, due to the stochastic and intermittent nature of renewable sources, several challenges make microgrids difficult to implement and maintain stable, on different scales: not only is the match between production and demand difficult to ensure, but also the quality of electricity must be carefully controlled due to frequency oscillations in the grid. [2] investigates the limit to the integration of renewables, highlighting the importance of energy storage with the case study of Corsica and reviewing different possible storage solutions for a hybrid PV/wind/hydro system with 30% RES penetration. Pumped hydro is proposed, when possible, as a good storage solution to help increase the renewable penetration in the system. The main concern expressed in the conclusions is the high cost of storage, which undoubtedly improves the performance but whose investments might not be justified in microgrids with a small size of the RES system. An important suggestion for the increase of RES penetration is to change the hypothesis of the energy management, and adopt more flexibles strategies for the thermal generators.

[7], [8] and [9] build a mixed integer linear programming model based on time series to determine the optimal design of a hybrid system with BESS, including PV, biomass, micro-hydro and a fossil backup. In these papers, the objective function to minimise is only the cost function, constrained by the demand/production match at hourly steps. The papers are very detailed with the equations modeling the system's components, which have in part been adapted to the purpose of this thesis. An extensive paragraph is dedicated to the possible operational strategies of the system, which have been a useful inspiration for this work. The conclusion of the papers is that not only can hybrid systems be cost effective, but they can also increase the grid reliability in rural areas, as demonstrated by many other papers such as [10].

To assess the long-term performance of a hybrid system, often related directly with the Expected Energy Not Supplied (EENS), [11] makes a distinction between two macro-branches: analytical methods, and simulation methods. The seconds, stochastic methods often regarded loosely and improperly as Monte Carlo Simulations (MCS), can be based on the energy balance over a time period, or more accurately on time series when data is available, or on probabilistic methods treating all variables involved as stochastic variables. The paper shows a detailed formulation of a probabilistic model, with a particular focus on cloudiness modeling for PV production estimation, applying the methodology on a case study in Stromboli island, Italy. The versatility of the probabilistic approach, especially when few data is available, has proven fundamental for a significant part of this thesis.

## 2.2. OPTIMISATION ALGORITHMS

A large part of the computational effort in the optimisation algorithm of this work is allocated to the Unit Commitment (UC) schedule for the thermal generators. Several models have been proposed in the last 60 years.

[12] perfectiones existing UC method and proposes a new approach based on dynamic programming, by decommitting units until cost can no longer be reduced without violating the spinning reserve constraints. Throughout a code in Fortran, the paper shows that this approach can converge to stable results in a more efficient time than Lagrangian Relaxation or Sequential Unit Commitment method. [13] proposes a UC method which also includes energy storage systems to achieve load levelling and reduce costs, by first compiling a Priority List and then applying the operational constraints.

[14] studies uncertainty in the UC problem, proposing the integration of stochastic methods into the traditional multi-stage approach. In general, UC is decided hours before the actual operation, using forecasts and projections of the load to choose which units to commit for each time step. Afterwards, short before the operation, when more uncertainties have been sorted out, the stage of Economic Dispatch (ED) takes place, to decide the actual power output needed from each unit to meet the real load. By elaborating a hybrid approach between commonly used reserve requirements and stochastic programming, the authors demonstrated that such methodology leads to increased flexibility and robustness in the solution, especially in the case of extreme events.

[15] also used stochastic programming, in a similar way as the approach used in this thesis, to determine the optimal UC in a HES with high wind penetration whose production is modeled through an Auto-

Regressive Moving Average (ARMA) model. As a result, stochastic optimisation proved to be more economical and better performing than the deterministic approach, leading to a reduced need for operating reserve in the system. [16] increases the complexity of this approach by using stochastic dynamic programming to solve the UC problem in HES with large wind capacity, whose output is described with a Markov chain-generated time series. Again, results show higher economic performance compared with both deterministic approaches and Monte Carlo derived simulation models.

Recenty, also several meta-heuristic algorithms have been developed, to deal not only with uncertainty but also with the multiple conflicting objectives to minimise in the problem, such as costs, renewables curtailment, loss of load probability, and $CO_2$ emissions. [17] uses a fuzzy self-adaptive Particle Swarm Optimisation (PSO) to optimise UC when load and wind uncertainties are present. Stochastic scenarios are generated with Monte Carlo Sampling and Roulette Wheel Mechanism. The proposed evolutionary algorithm uses fuzzy adaptive weight factor to avoid remaining stuck on local optima, and a new sel-adaptive learning operator to improve the speed and performance of the code. In addition, the multi-objective approach has the benefit of allowing the decision maker to update the tradeoff between the conflicting objective as preferred.

[18] uses again PSO, for its simplicity and effectiveness and its ability to deal with non-linear and non-continuous problem where gradient-based methods would fail. The system to optimise, together with a BESS, also involves a fuel cell, an electrolyser and a hydrogen storage tank.

On the other hand, [19] uses probabilistic methods to solve the UD problem, using probability density function to describe wind power generation, jointly with the probability of a failure event in the thermal units. The approach is compared to Monte Carlo simulation, and has proven to yield good quality results especially when failure events in generation units are neglected. The methodology is further perfectioned in [20] and combined with Priority List method, demonstrating to be a simple approach to get acceptable results, although not as accurate as the PSO optimisations, more suitable for the industrial purposes.

Several other hybrid renewable microgrid optimization techniques are reviewed in [21], including Artificial Intelligence, Genetic Algorithms (GA), Fuzzy Logic and Artificial Neural Networks. Some of these methaeuristic methods, specifically GA and PSO, have been succesfully applied to the Terceira island case study in [22] to find the optimal configuration of a Water Pumped storage system for a HES.

## 2.3. AZORES' ENERGY CHALLENGES

As previously mentioned, challenges in microgrids are many and not easy to face. Storage systems are only one of the potential solutions, and many studies demonstrated that isolated hybrid energy systems are a good field for sperimentation of new technologies such as demand-response optimisation or vehicle-to-grid (V2G) applications. In particular, several recent papers analysed the potential of new energy technologies to face the energy challenges in the Azores.

[23] modifies a UC+ED model to determine the optimal BESS size to provide spinning reserve and to reduce the load on thermal generators in Terceira. The BESS is only charged with curtailed RES to improve the usage of the energy produced by renewable generators. Two objectives are alternately

pursued, to minimise the curtailment and to maximise the NPV. In both cases, positive NPVs are reached by model, for a resulting BESS capacity between 2380 kWh and 6300 kWh.
Also [24] deals with BESS integration, by developing a multi-stage optimisation based on Mixed Integer Linear Programming and testing on a case study in the Azores archipelago. The paper shows the technical and economical benefits of energy storage in the islanded system, which helps lowering operating costs during the 15-year project horizon and reducing wind energy curtailment.

[25] and [26] tackle microgrid challenges with different approaches, throughout demand-response optimisation. A modified ED model previously developed for Corvo island is used in [25] to analyse a case study in Terceira, in which the flexible loads are shifted and optimised combining linear programming with a genetic algorithm. Consumers are assumed to be prosumers, and the introduction of self-consumption systems makes an extra step towards the recent concept of a smart grid. The approach showed to reduce production costs and renewable shares, at the same time reducing the peak load.

[27] analyses the benefits of introducing electric vehicles on the energy system of Flores island. Only flexible recharge strategies demonstrated to improve the exploitation of RES, while fixed recharge times increased the load on thermal generators in the adopted simulation. Nevertheless, a good control strategy on the EV's electric load proved to be able to reduce $CO_2$ emissions in the island and to help increase the sustainability of the energy system, although requiring a strong support from policies and economic incentives in order to become feasible on large scale.

[28] assesses the benefits on Terceira's grid of a Water Pumped Storage System (WPSS). Despite using a simplified model instead of a real optimisation technique, the results showed that not only WPSS can reduce the need for SR and facilitate the integration of RES, but also that it can do it in an economically viable way. Nevertheless, as will be highlighted later in this thesis, also this work clashed with the quite rigid SR requirements of the grid operator in the Azores, which make SR redundant when other storage systems are present. Such requirements should be reconsidered by EDA, since they significantly limit the renewable penetration in the system by forcing RES curtailment.

[29] performs a Life Cycle Assessment of electricity generation in Graciosa, analysing the ambitious project announced in 2015, of a hybrid wind/PV/Li-Ion BESS microgrid with high RES penetration, up to 65%. As a result, according to the paper the project leads to a reduction of 43% of environmental impacts, with more than 60% of the residual impacts still being due to the remaining thermal generators. Again, the increase of storage capacity is suggested to reduce RES curtailment.

# 3. METHODOLOGY

This chapter describes the simulation model proposed in this thesis and the optimisation algorithm implemented in MatLab and used to determine the optimal configuration of the HES in different scenarios. A particular focus is dedicated to the UC strategy and to the calculation of the financial parametres of the project.

## 3.1. SIMULATION MODEL

The HES in this work is a network of several components, whose proposed configuration is shown in Figure 1. The renewable part of the system is composed by wind turbines, a geothermal power plant and photovoltaic arrays. Diesel engines provide spinning reserve and fulfil the load-following role in the system, together with the energy storage system. In the Faial case study this have been assumed to be Li-Ion batteries for their quick response, but in general this model does not put any constraints against other sources of storage such as flywheels or pumped water systems. Both batteries and thermal generators are used as regulatory reserve for frequency stabilisation, and it is important to ensure that the system is able to adapt to the load on different time levels, from a very short time span, using batteries for frequency regulation, to longer time spans using storage and gensets to level oscillations [30].

As shown in the scheme in Figure 1, the system has an AC bus to which wind, geothermal and diesel generators are connected, and interfaced directly with the grid and the loads. At the same time, a rectifier allows the possible power production excess to be stored in the battery, through a charge controller, or to be curtailed. The PV arrays are connected directly to the charge controller, which manages the power flows between PV array and battery and the inverter which interfaces the DC bus with the grid.

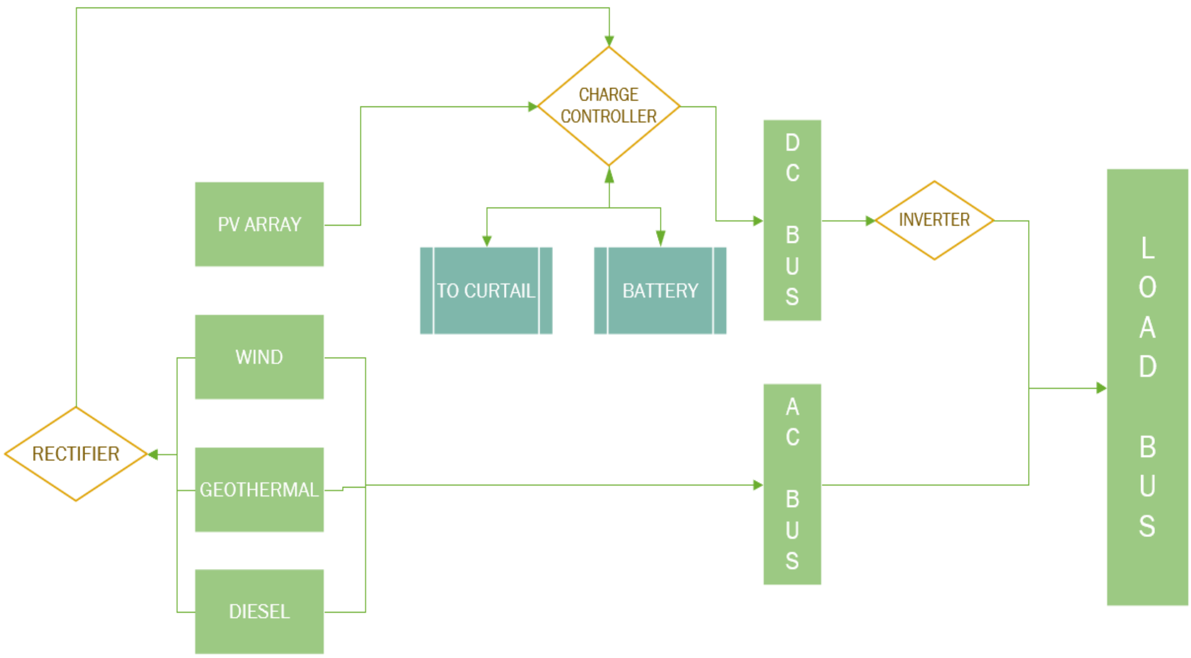


**FIGURE 1 – LOGICAL SCHEME OF THE SYSTEM**

Since five wind turbines are already installed in the island, the assumption has been made that the model used the same turbine model, Vestas V52/850, to calculate the power production not only for the turbines already present but also for any new turbine which the optimisation suggested to install. The cut-in and cut-off speeds are 3 m/s and 25 m/s respectively, while the rated speed is 14 m/s. Consequently, between rated speed and cut-off speed the turbines produce at their nominal power output, 850 kW. Between cut-in and rated speed, the output follows the power curve of the turbine, given by the producer as discrete values at intervals of 0.5 m/s of wind speed and shown in Figure 2 [31]. For intermediate values, the output power is obtained by shape-preserving piecewise cubic (PCHIP) interpolation. Hub height of the turbines has been assumed as 100 metres.

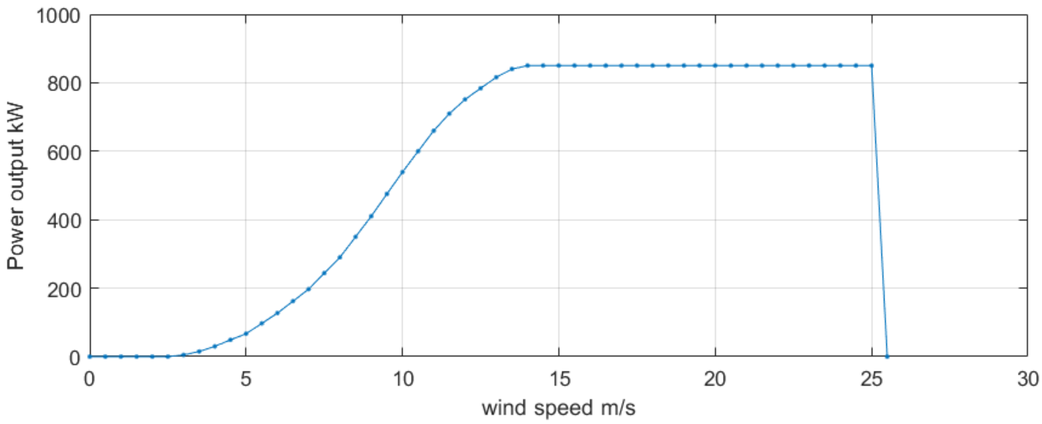


**FIGURE 2 – POWER CURVE OF VESTAS V52/850 [31]**

The energy produced by PV panels is directly proportional to the solar irradiation, and has been calculated using the HDKR model, as explained in detail in chapter 5.3. Power output from geothermal plants has been considered constant, and equal to the nominal installed capacity of the plant.

The energy generated from renewable sources in a time step is then defined as:

$$E_{RES} = E_{wind} + E_{PV} + E_{geo} \tag{1}$$

The simulation model, written in MatLab as a function called *objfun*, receives inputs from three *.m* files, containing respectively the hourly demand, the hourly average wind speed (HAWS) and the specific electric production in $W/m^2$ of PV panels installed. The last is afterwards converted in electric production per panel, in order to discretise the result to an integer number of panels. After these input data have been loaded, the RES power generation for each time step is calculated with equation (1).

Then the required spinning reserve (SR) is calculated according to its definition. In the case study of Faial SR is related to the wind speed, as common practice by EDA [22], and its definition is reported in equation (38) in section 5.5. If the sum of the energy produced by RES and SR exceeds the load, the excess is stored in battery or, if the battery is full, part of the RES generation is curtailed. Otherwise, if additional power is still needed, a Unit Commitment (*UC*) model is called from a separate function to determine the optimal dispatch and power output of the thermal engines to match the remaining load, and the respective cost.

This strategy is described by the following equations, starting with the calculation of the energy flow managed by the charge controller between the RES array and the battery:

$$E_{to}^{BESS} = (E_{RES} + E_{SR}) - E_{load} \quad (2)$$

Where $E_{to}^{BESS}$ is the energy sent or requested from the battery, depending if such value is greater or smaller than zero respectively. At this point, the energy theoretically present inside the battery $E_{into}^{BESS}$ amounts to:

$$E_{into}^{BESS} = C_B \cdot SoC_{bop} + E_{to}^{BESS} \cdot \eta_{BESS} \quad (3)$$

Where $C_B$ is the capacity of the battery, which coincides with the decision variable $x_4$, $SoC_{bop}$ is the state of charge of the battery at the beginning of the period, expressed as a value from 0 to 1, and $\eta_{BESS}$ is the efficiency of the battery, which in first approximation has been assumed to be the same for charge and discharge. So far, $E_{into}^{BESS}$ does not take into account the limits of minimum and maximum energy that can be stored, which are imposed by the definition of the state of charge at the end of the time step, $SoC_{eop}$:

$$SoC_{eop} = \begin{cases} 1 & if \ \frac{E_{into}^{BESS}}{C_B} > 1 \\ \frac{E_{into}^{BESS}}{C_B} & if \ SoC_{min} \leq \frac{E_{into}^{BESS}}{C_B} \leq 1 \\ SoC_{min} & if \ \frac{E_{into}^{BESS}}{C_B} < SoC_{min} \end{cases} \quad (4)$$

Equation (4) encompasses all the possible behaviours of the battery, charging or discharging inside its operational range, or reaching its upper or lower limit of charge, respectively 1 and $SoC_{min}$. In case the battery is full, part of the energy sent to the battery must be dissipated; the energy that the charge controller curtails has been defined as:

$$E_{curt} = \begin{cases} E_{into}^{BESS} - C_B & if \ SoC_{eop} = 1 \\ 0 & else \end{cases} \quad (5)$$

On the other hand, the amount of energy discharged by the battery, $E_{disch}^{BESS}$, is:

$$E_{disch}^{BESS} = \begin{cases} (SoC_{bop} - SoC_{min}) \cdot C_B \cdot \eta_{BESS} & if \ \frac{E_{into}^{BESS}}{C_B} < SoC_{min} \\ \max(-E_{to}^{BESS} \cdot \eta_{BESS} \, ; 0) & else \end{cases} \quad (6)$$

where the subscripts *bop* and *eop* indicate the beginning of period and end of period of each time step. Finally, the remaining load to be supplied by the thermal generators, $E_{thermal}$, is computed:

$$E_{thermal} = E_{load} - (E_{RES} + E_{SR} + E_{disch}^{BESS}) \quad (7)$$

The value of $E_{thermal}$ is sent to the UC function to determine whether it is feasible to provide by the thermal generators, and with which optimal dispatch of the gensets. To shorten the execution time, the user of the model can choose to bypass the UC model during the optimisation, by simply using a linear function for cost as explained more in detail in section 5.4, and use the UC model only in the optimum solution after running the optimisation, to check if there are any unfeasible states.

In case the thermal generators are used below their minimum load point, the generation is forced to increas up to that point, and the behaviour of the battery is recalculated:

$$if \ E_{SR} + E_{thermal} < C_{min}^{therm} \rightarrow E_{thermal} = C_{min}^{therm} - E_{SR} \quad (8)$$

$$E_{to}^{BESS} = (E_{RES} + E_{SR} + E_{thermal}) - E_{load} \tag{9}$$

At the same time, the sum of SR and the rest of thermal generation must be lower or equal to the installed capacity of the generators $C_{therm}$, 19100 kW in the case of Faial:

$$if\ E_{SR} + E_{thermal} > C_{max}^{therm} \rightarrow E_{thermal} = C_{max}^{therm} - E_{SR} \tag{10}$$

At the end of this, the time step is solved and the simulation passes to the next one. The process is repeated for every hour of the year; at the end, *objfun* calculates the total energy produced by the generators of each type, and computes the Renewable Energy Fraction ($REF_{min}$) and the Energy Index of Reliability ($EIR_{min}$) of the system. These parametres are defined as follows:

$$REF = \frac{\sum E_{RES} - \sum E_{curt}}{\sum E_{load}} \tag{11}$$

$$EIR = 1 - \frac{EENS}{\sum E_{load}} \tag{12}$$

Where $E_{RES}$, $E_{curt}$ and $E_{load}$ are respectively the energy produced from RES, the energy curtailed and the energy demand at each hourly time step, and $EENS$ is the total Expected Energy Not Supplied at the end of the period considered:

$$EENS = \sum_{8760} [E_{load} - (E_{RES} + E_{SR} + E_{disch} + E_{thermal})] \tag{13}$$

This parametre becomes different from zero when the low available capacity of thermal generators of their ramp up and down constraints prevent them from succesfully following the load. Anyway, despite the model being able to support more general cases, in the present work such ramp constraints have been neglected, and the EIR is almost always equal to one.

Finally, the NPV of the system is calculated according to the definition in equation (28) in section 3.4, where this process is described in detail. The NPV represents the actualised value of all the net income cash flows generated by the project, plus the residual value of the installations at the end of their nominal 20 years lifetime.

## 3.2. OPTIMISATION MODEL

The optimisation model has been developed in MatLab, based on the *fmincon* engine for constrained objective function minimisation. The decision variables are the installed capacities of wind, solar and geothermal generators in kW, as well as the storage capacity in kWh, while the installed power of the thermal generators is fixed and coincides with that already present in the system.

Since the decision variables come in the form of an array $x$, later in this work they are also referred to as follows:

$$x = \begin{pmatrix} x_1 \\ x_2 \\ x_3 \\ x_4 \end{pmatrix} = \begin{pmatrix} wind\ [kW] \\ PV\ [kW] \\ geothermal\ [kW] \\ storage\ [kWh] \end{pmatrix} \tag{14}$$

The objective function to maximise is the compared Net Present Value (NPV) of the system over 20 years, which is simply the difference between the NPV of the configuration under study and the NPV of the current configuration of the system, as explained more in detail at the beginning of chapter 6.

To cope with the multi-objective nature of the theoretical problem, the secondary objectives have been introduced as variable linear and non-linear constraints, simplifying the problem into a single-objective constrained optimisation. In particular, lower (LB) and upper bounds (UB) to the decision variables can be customised, and minimum values for the Renewable Energy Fraction ($REF_{min}$) and the Energy Index of Reliability ($EIR_{min}$) can be imposed.

The constraints can be described as:

$$\begin{cases} LB \leq x \leq UB \\ REF \geq REF_{min} \\ EIR \geq EIR_{min} \end{cases} \tag{15}$$

For computational power limitations, the model operates at hourly time steps for one year. The environment conditions and energy production are assumed to remain constant for the rest of the system's lifetime.

The algorithm starts from an initial guess of the decision variables, $x_0$, and iterates on it towards an optimal solution until the steps in the values of the variables and of the objective function become too small to be significant. The non-linear constraints of $REF_{min}$ and $EIR_{min}$ are defined in a separate function, *nonlincon*, that receives the values of the constrained variables which are calculated by *objfun* at every iteration. The objective function represents the simulation model: it contains the energy model and the calls to the UC model and the financial model, and can be run independently from the optimisation algorithm in case only a single scenario has to be simulated.

Finally, the values of the decision variables in the iteration, the total yearly cost for thermal engines, the energy production and the $CO_2$ generation are passed to a function containing the financial model, which calculates in detail the NPV of the project. When the decision variables converge to an optimal result, an Excel sheet is printed with the hourly breakdown of the energy balance, the values of the decision variables, the investment and operational costs for each component, the NPV (and Internal Rate of Return IRR when positive) of the equity and of the project, compared with the current system, the EENS, EIR and REF.

## 3.3. Unit Commitment and Economic Dispatch

Because of the complexity of the task, an existing UC model has been extracted from [32] and modified to be adapted to the model and to perform some extra calculations. The function, based on the approach from [33], treats the problem deterministically using a forward dynamic programming algorithm. Minimum up and down times and generators' ramp constraints have been neglected for simplicity, also considering that in a small islanded system with small size generators such constraints would not be particularly significant.

The logic behind this multi-stage algorithm is simple. The starting point is the known state at the previous hour, where committed and non-committed generators are represented by Boolean logic operators. Then, for every following hour, the program finds all the potentially feasible states, and for each of them evaluates if also the transition from the previous state is feasible. At this point, economic dispatch consists in choosing the path with the lowest cost, considering both start-up costs and operation costs. Shutdown cost has been assumed as negligible again due to the small size of the generators. The simplified mathematical formulation of this problem is the following:

$$\min\left(\sum_t \sum_i (Cost_{t,i} + StUp_i)\right) \quad (16)$$

In formula 16, $Cost_{t,i}$ is the operating cost of generator $i$ at time $t$, expressed as a quadratic function of the power output in the same instant through three coefficients $a, b, c$:

$$Cost_{t,i} = a + b \cdot P_{MWt,i}^{therm} + c \cdot \left(P_{MWt,i}^{therm}\right)^2 \quad (17)$$

Such coefficients are usually provided by the producer. In the case study of Faial, their origin is more detailedly explained in section 5.4

As for the transitions, the cases can be summarised as in Figure 3:

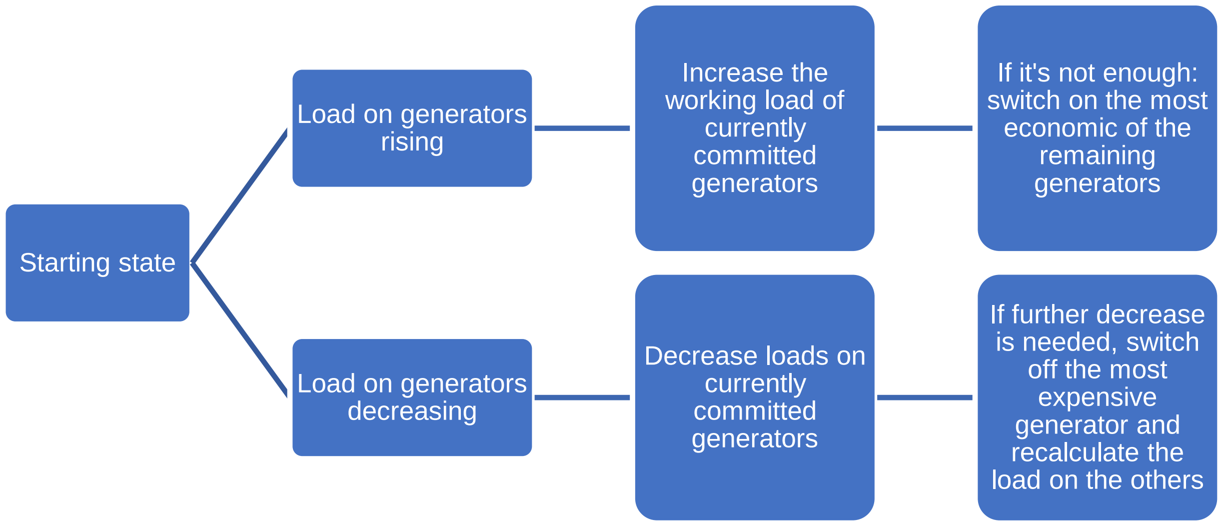


**Figure 3 – Logical scheme of UC model**

## 3.4. FINANCIAL MODEL

The financial model takes as inputs the installed capacities of the system, the fuel consumption in one year, the overall energy produced and the $CO_2$ emissions to calculate possible carbon taxes. Then, the NPV is calculated and returned as an output, by elaborating in parallel the income statement with profit and loss and the cash flows statement, to account accurately for the taxes, the depreciation and the time value of money.

The Earning Before Interests, Taxes, Depreciation and Amortisation (EBITDA) is calculated as follows:

$$EBITDA = Income - CAPEX - Insurance\ costs - (fuel\ cost + O\&M + carbon\ tax) \tag{18}$$

Then interests are calculated, considering that a percentage of the investment (*credit*) is financed through debt. For all the years in the project lifetime, the function calculates the debt remaining at the beginning of the period (BOP) (the so-called *outstanding principal*), on which interest $Int$ is calculated as follows:

$$Int = Debt_{BOP} \cdot r \tag{19}$$

Then, the debt remaining at the end of the period (EOP) is:

$$Debt_{EOP} = Debt_{BOP} + Int - credit \cdot CRF \tag{20}$$

Where CRF is the Capital Recovery Factor, to calculate the annuity needed to estinguish the debt in 20 years:

$$CRF = \frac{r(1+r)^{20}}{(1+r)^{20} - 1} \tag{21}$$

In fact, the reduction in the debt after each period, called principal repayment, is the difference between each annuity and the passive interests accumulated over that period, which varies depending on the oustanding principal. In fact, the annuity first covers the interests on the period, and only then starts repaying the actual debt.

$$Principal\ repaymet = CRF \cdot credit - Int \tag{22}$$

Afterwards, depreciation needs to be calculated, since it is tax-deductible. In this specific model, accelerated depreciation over 5 years has been assumed, to take advantage of fiscal incentives as much as possible. Therefore, the depreciation is divided into two components. The first part, $depr$, is discounted from the taxes as much as this is possible. Then, since the project can not use all the depreciations due to its low pre-tax profit, the remaining part of depreciation $depr_{rem}$ is calculated, and the correspondant tax exemption is included as an income. In fact, such remaining depreciation will be cumulated with depreciation in other projects or operations of EDA and accounted as deductible from taxes.

When depreciation has been determined over the years, the income statement can be finished:

$$EBIT = EBITDA - Int - depreciation \tag{23}$$

The amount of taxes that it is necessary to pay is:

$$Taxes = EBIT \cdot tax\ rate \tag{24}$$

And finally:

$$Net\ Income = EBIT - Taxes + depr + depr_{rem} \cdot tax\ rate \tag{25}$$

On the other hand, since these economic calculations do not take into account the financial situation of the project, to calculate the NPV it is necessary to calculate the cash flows statement starting again from the EBITDA, and calculating the operating CF by removing the taxes from it. Then the variation in the outstanding principal is taken into account:

$$CF_{\Delta\,\mathrm{principal}} = credit - principal\ repayment \tag{26}$$

The cash flows related to debt correspond to the variation in the outstanding principal, plus the accumulated interests, accounted as a negative cash flow. As well as that, CF relative to the tax benefit derived from the remaining part of depreciation can be recalculated. the If the debt CF are subtracted from the opeating CF, and then the tax benefit CF is added, the Free Cash Flows to Equity are obtained, which represent the cash flow available to the company's common stockholders.

Afterwards, the function calculates the Net Operating Profit After Tax, which represents the company's earning if its capitalization were unleveraged, which means, if the project was funded by equity only, without debt.

$$NOPAT = (EBITDA - depr) \cdot (1 - tax\ rate) + depr \tag{27}$$

Finally, the free cash flows to project are computed, summing up the investment CF, the NOPAT, and the tax benefit CF from remaining depreciation. The free CF to project are the equivalent of the free cash flows to firm (FFCF), which are the cash flows available to all the providers of firm of the company.

The free cash flows to equity and to project are actualised with the Weighted Average Cost of Capital (WACC) and summed up with the residual value $rv$ discounted with the inflation rate (Consumer Price Index CPI at year 20) to calculate the NPVs of the equity and of the whole project. The equation that follows reports only the formula of the NPV of the project, since it is the value used as objective function. The NPV of equity follows a formally identical expression, but its value has only been used as a control value while debugging the code of the model.

$$NPV_{project} = \left( \sum_{y=1}^{20} \frac{FCFF}{(1 + WACC)^y} \right) + rv \cdot CAPEX \cdot CPI_{20} \cdot \frac{1 - tax\ rate}{(1 + WACC)^{20}} \tag{28}$$

The difference between the latter and the NPV of the current configuration is the value which has been used as objective function to maximise.

# 4. The Faial Case Study

Açores is a Portuguese archipelago of nine volcanic islands in the Atlantic ocean, around 1400 km West of the coasts of Portugal. The islands are significantly distant from each other; the two farthest ones, Santa Maria and Corvo, are around 600 km far from each other. For this reason, every island is energetically independent from the others, and presents its own independent grid.

Due to their position in correspondance of a junction between three tectonic plates, the area presents a large geothermal potential, already partially exploited. Wind parks and micro-hydro power plants with seasonal character are present as well, while the solar resource is currently almost unused. Because of the need for grid stability, however, all islands have a variable dependency on fossile fuel generators, as visible in Figure 4, ranging from 53.9% in São Miguel, the largest island, to 100% in Corvo and Graciosa, the two smallest ones.

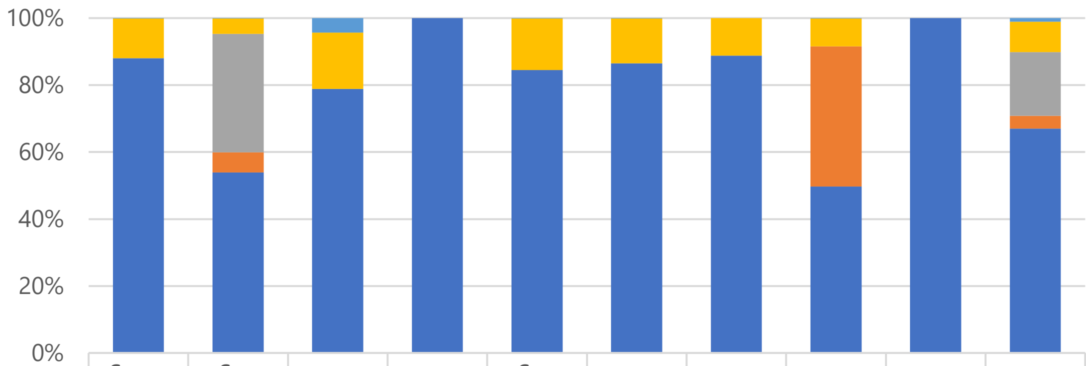


| | Santa Maria | Sao Miguel | Terceira | Graciosa | Sao Jorge | Pico | Faial | Flores | Corvo | Açores |
|---|---|---|---|---|---|---|---|---|---|---|
| Other | 0,1% | 0,1% | 4,3% | 0,0% | 0,1% | 0,1% | 0,0% | 0,1% | 0,0% | 1,1% |
| Wind | 11,9% | 4,6% | 16,8% | 0,0% | 15,4% | 13,4% | 11,2% | 8,3% | 0,0% | 9,1% |
| Geothermal | 0,0% | 35,4% | 0,0% | 0,0% | 0,0% | 0,0% | 0,0% | 0,0% | 0,0% | 19,0% |
| Hydro | 0,0% | 6,0% | 0,0% | 0,0% | 0,0% | 0,0% | 0,0% | 41,9% | 0,0% | 3,8% |
| Diesel | 88,0% | 53,9% | 78,9% | 100,0% | 84,5% | 86,5% | 88,8% | 49,7% | 100,0% | 67,0% |

**Figure 4 – Electricity production mix in the Azores in 2016 [34] [35]**

Overall, the electricity mix in the Açores is more fossil-based than the continental one. Carbon emissions in the archipelago amount to roughly 2 million tons of $CO_2$ per year, of which 73% from energy production [36].

The island of Faial, belonging to the central group of the Açores, is the third most populous island in the archipelago after São Miguel and Terceira. In its 173 km$^2$, Faial was home to 14.759 inhabitants at the end of 2016 [37], around 6% of the total Açores population. The island belongs to the central group of the Açores, together with São Jorge and Pico as well as Graciosa and Terceira; the first three three islands are the closest to each other in the archipelago.

## 4.1. ENERGY SYSTEM IN FAIAL

The energy system in the island of Faial is characterised, as visible in Figure 5, by mainly domestic and commercial users, on a scale which is small enough not to require a high voltage (HV) transport grid, so that only a distribution grid is present. According to EDA, at the end of December 2017 there were 8108 users on the island [38]. The power generation is ensured by the Wind Park of Salão, the Hydroelectric power plant of Varadouro, and the Thermoelectric plant of Santa Barbara. The island relies heavily on this last one, as shown further on in Table 1 and in Figure 7; for this reason, Faial is the island with the third highest specific emissions (643.65 $g_{CO2}$/kWh in 2017), after Corvo (719.89 $g_{CO2}$/kWh) and Graciosa (690.12 $g_{CO2}$/kWh) [39]. For a comparison, the average specific emissions in overall Portugal in 2017 have been 198.5 $g_{CO2}$/kWh, less than one third of Faial's [40].

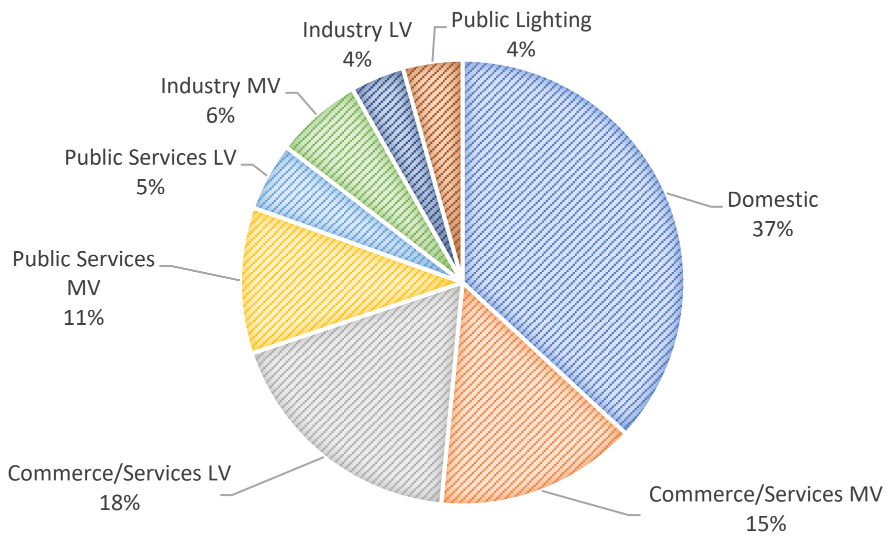


**FIGURE 5 – BREAKDOWN OF ELECTRICITY CONSUMPTION IN DECEMBER 2017 IN FAIAL [38]**

Electricity production in 2016 amounted to 43329 MWh and total sales of electricity to 7.055.945€, for an average price of 162.85 €/MWh. This is the retail price which has been used in the model presented in this work, specific for Faial and not far from the average 2016 retail price of electricity in the Azores, which was 15.74 c€/kWh [41].

As can be seen in Figure 6, Faial's electric system is quite simple and not very large, which justifies some of the simplificative assumptions used in the model and the input data of this thesis, such as the unitary efficiency for the transmission lines.

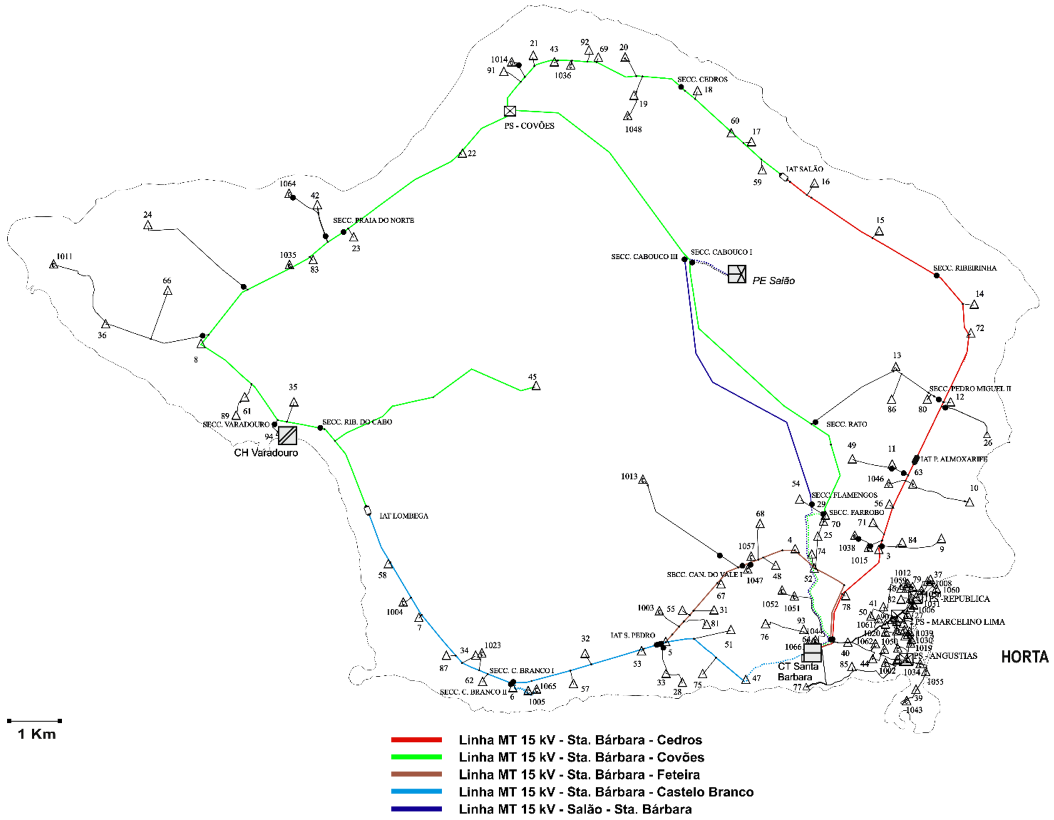


**Figure 6 – Map of electric grid in Faial [34]**

In the same map it is possible to see the main generation plants on the islands. The thermal plants (with the symbol CT on the map, for *Central Térmica*) are all located near Horta, while the Salão wind park (PE; *Parco Eolico*) is at the north-east of the *caldeira*, the volcanic mountain at the centre of the island, and the hydroelectric plant of Varadouro (CH, *Central Hidroeletrica*), is along the west coast.

The energy flows are managed by the control system from ABB [42], a sophisticate Renewable Microgrid Controller (RMC) able to automatically set the operating conditions of all generators to optimise the wind power utilisation. The RMC is designed to allow control flexibility and to be suitable for modifications in the system and future increases of renewable installed capacity. Furthermore, it has the ability to interface also with potential future storage systems.

**Table 1 – Electricity monthly production in Faial in 2017 [39]**

| | DIESEL | | WIND | |
|---|---|---|---|---|
| | MWh | % | MWh | % |
| *JAN* | 3821 | 91,8% | 340 | 8,2% |
| *FEB* | 3341 | 90,7% | 344 | 9,3% |
| *MAR* | 3556 | 89,0% | 441 | 11,0% |
| *APR* | 3469 | 92,2% | 294 | 7,8% |
| *MAY* | 3661 | 92,2% | 311 | 7,8% |
| *JUN* | 3629 | 92,5% | 296 | 7,5% |
| *JUL* | 4206 | 94,2% | 258 | 5,8% |
| *AUG* | 4438 | 95,0% | 235 | 5,0% |
| *SEP* | 4027 | 90,9% | 404 | 9,1% |
| *OCT* | 3666 | 85,7% | 611 | 14,3% |
| *NOV* | 3288 | 83,4% | 655 | 16,6% |
| *DEC* | 3495 | 86,3% | 554 | 13,7% |
| ***TOTAL*** | 44597 | 90,3% | 4743 | 9,7% |

The hydro plant of Varadouro, with an installed power of 320 kW, follows the seasonal hydrological nature of most rivers of the Açores. However, because of the last years' drought there has not been any production in 2016 and 2017, as can be also seen in Table 1.

As for the Parque Eólico do Salão, its origin dates back to 2002, when Wind Park *da Lomba dos Frades* was built in the context of the *Plano de Desenvolvimento de Energia Eólica dos Açores*. Such wind park counted 6 ENERCON E-30 aerogenerators of 300 kW and was the first experience of EDA to integrate wind systems with the thermal production based on fuel oil. It was then dismantled in 2011 because of protests from residents nearby, which limited the time availability of the turbine such that the production of the wind park was less than a half of the expected one [43] [44]. The new wind park that replaced it in 2013 in the north of the island aims at covering 20% of the island's energy demand [45] [31] [46]. It features 5 Vestas V52/850 turbines, of 850kW each for a total of 4.25 MW of installed power and an investment of over 6 million Euros.

Finally, the thermal plant of Santa Barbara, which represents the main energy source of the island with its 19.1 MW of capacity, features six heavy fuel oil (HFO) generators, whose details are summarized in Table 2.

**TABLE 2 – SUMMARY OF FUEL GENERATORS IN FAIAL**

| NAME | MODEL | VOLTAGE [kV] | POWER [kW] (PF = 0.8) | TECHNICAL MINIMUM (50%) |
|---|---|---|---|---|
| **G3** | Sulzer 6ZL 40/48 | 10 | 3000 | 1500 |
| **G4** | Sulzer 6ZL 40/48 | 6,6 | 3000 | 1500 |
| **G5** | Krupp MAK 6M4 53C | 6 | 2000 | 1000 |
| **G6** | Caterpillar/MAK 8C M32C | 6,6 | 3705 | 1853 |
| **G7** | Caterpillar/MAK 8C M32C | 6,6 | 3705 | 1853 |
| **G8** | Caterpillar/MAK 8C M32C | 6,6 | 3697 | 1849 |
| **TOTAL** | | | **19107** | **9555** |

## 4.2. TRENDS IN ELECTRIC PRODUCTION AND CONSUMPTION

As shown in Figure 7, a clear trend for energy demand in Faial can not be identified from the available data. For this reason, in the model in this thesis it has been assumed that the load does not tend to grow or to decrease in the years, but it just oscillates around an average value, with a standard deviation of around 4% calculated from the data sample obtained from EDA's archives.

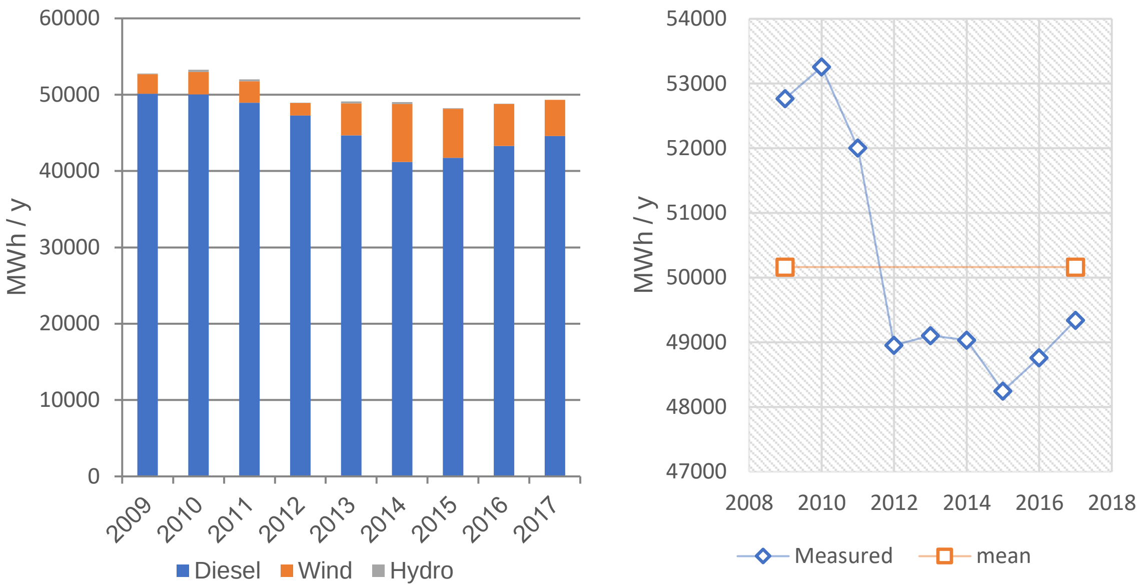


**FIGURE 7 – TOTAL ENERGY PRODUCTION IN FAIAL IN YEARS 2009 – 2017 [39]**

From the same dataset it is possible to observe how variable and uncertain the production from renewables is, as plotted in Figure 8. In particular, the production of the hydro plant is highly unreliable and, when present, is a negligible share of the yearly production in the island. For these reasons, for simplicity hydropower has been excluded from the model presented in this work.

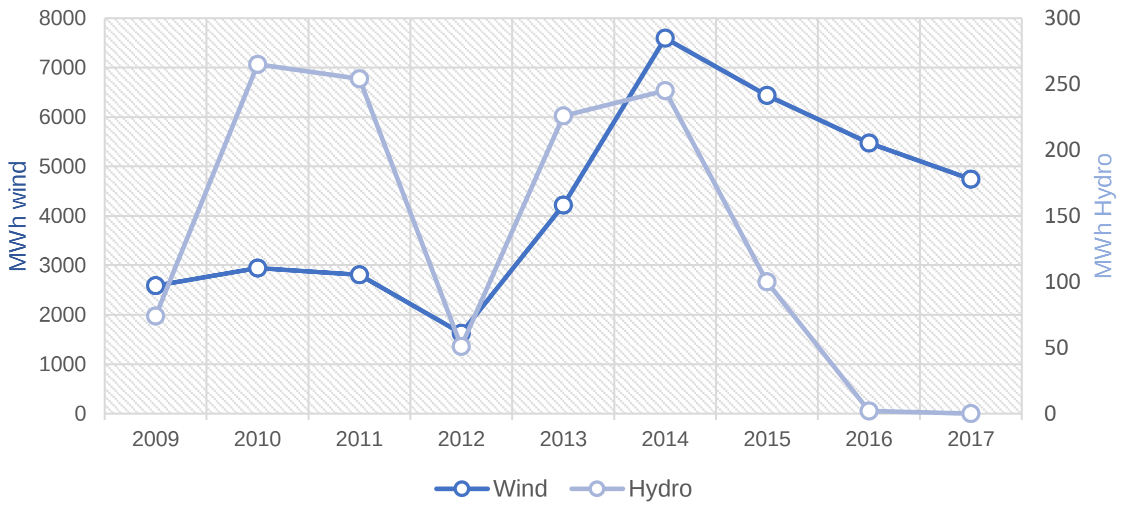


**FIGURE 8 – WIND AND HYDRO ELECTRICITY GENERATION IN YEARS 2009 - 2017 [39]**

# 5. Input data and synthetic time series generation

As previously mentioned in section 2.2, the model in this thesis works with stochastic scenarios as inputs, based on probability distributions fitted to real data and generated with algorithms following a logic similar to what presented in [17]. Stochastic methods increase the robustness of the solution, as well as the integration of the spinning reserve constraints, as demonstrated by [14].

This chapter describes how scenarios have been generated and how input data have been collected, elaborated and adapted to be used by the MatLab model.

## 5.1. Electricity demand

The data for electricity demand have been made available by EDA for only four days, precisely the 20th day of January, April, July and October of 2017, with intervals of 30 minutes, as illustrated in Figure 9.

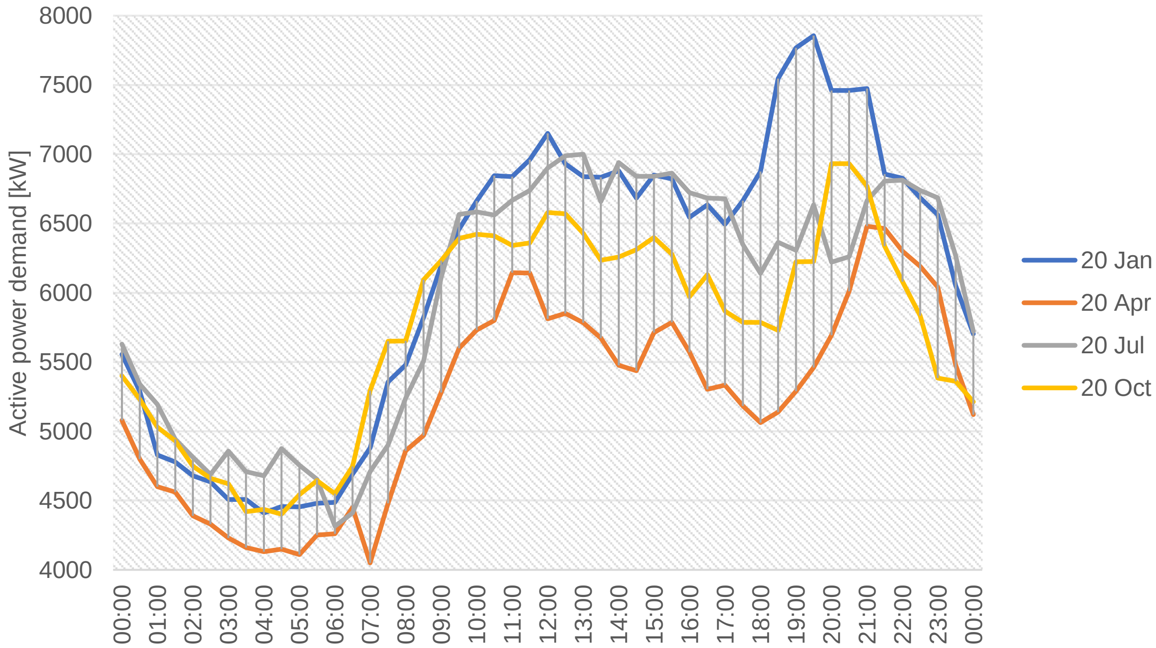


**Figure 9 – Sample of load curves measured by EDA in 2017**

Load curves for every other day has been generated with Monte Carlo sampling: every needed hourly demand value of any day of the year has been expressed as a normal probability distribution. As mean, the distribution uses the mean of the load values at the same hour of the two nearest days between the ones provided by EDA. As standard deviation, their semidifference of the same values was used. As an example, indicating with $L_{may8}^{13}$ the load in kW between 13h and 14h on the 8th of May, and with $\mu$ and $\sigma$ the mean and standard deviation of its probability function:

$$\mu_{may8}^{13} = \frac{L_{apr20}^{13} + L_{jul20}^{13}}{2} \tag{29}$$

$$\sigma_{may8}^{13} = \frac{\left|L_{apr20}^{13} - L_{jul20}^{13}\right|}{2} \tag{30}$$

In this way, random yearly demand curves with hourly values can be generated, respecting the statistical trends that link them with realistic scenarios, while at the same time allowing the presence of a few outliers. Such values represent situations that are highly unlikely to happen but not impossible, and are therefore useful to test the resilience and the ability of the energy system to deal with those situations. Figure 10 is a graphical representation of one of these synthetic time series, where every line of a different colour represents one day of the year.

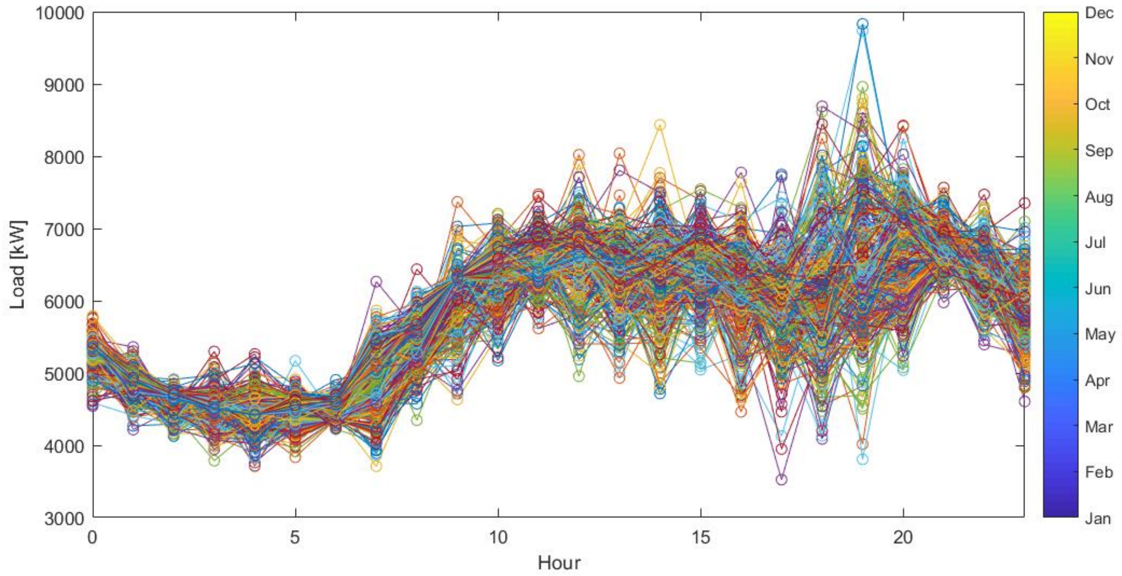


**FIGURE 10 – PLOT OF A HOURLY LOAD CURVE OBTAINED WITH THE STOCHASTIC APPROACH**

Also, the possibility of generating an unlimited number of yearly load curves at hourly steps has proven to be useful to verify, at the end of the optimisation, the suitability of a system design to cope with the possible situations that may arise over the years.

## 5.2. WIND SPEED

Data regarding wind speed and direction have been made available by EDA for the year 2017 only, at intervals of 10 minutes and at two different heights (20m and 47m from ground). Such data comes from a measurement station installed in *Alto do Cabouco*, a hill in the North-East of Faial not far from Salão, at an altitude of 514 metres. To estimate the wind speed at hub height, logarithmic wind profile has been assumed:

$$U(z) = k \cdot ln\frac{z}{r} \tag{31}$$

Where $U(z)$ is the wind speed at height $z$, $k$ is a constant, and $r$ is the terrain roughness parameter. The last has been calculated by replacing in the equation above known pairs of values of wind speed at different heights. Since 10-minute interval in the data provided by EDA represents a pair of values at the two heights, for increased accuracy a roughness value for every hour has been searched by using MatLab's solver *fsolve*. Then, an average on all the hours when a solution could be found has been calculated, and the resulting value of roughness $r = 0.0665$ has been used in the logarithmic profile function to calculate hourly wind speed at hub height.

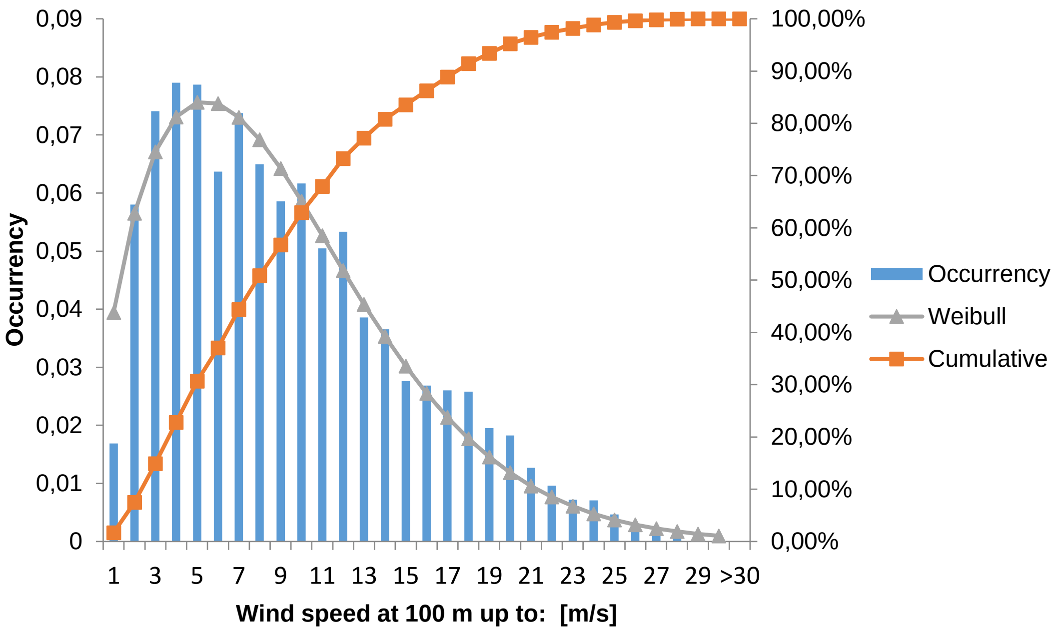


**FIGURE 11 – HISTOGRAM OF ESTIMATED WIND SPEEDS FOR YEAR 2017, AT HEIGHT OF 100 METRES**

As visible in Figure 11, wind speed occurrency can be well described by a Weibull distribution with a shape parametre β = 1.5937 and a scale parametre η = 10.0247. Such fit has a R-squared value of $R^2$ = 95.24% which is indicative of a good accuracy of the probability curve estimation. The equation of the Weibull distribution is defined as follows:

$$We(x) = \frac{\beta}{\eta^{\beta}} x^{\beta-1} \cdot e^{-\left(\frac{x}{\eta}\right)^{\beta}} \tag{32}$$

The influence of wind direction has been disregarded.

It is possible to assume that wind speed always follows the probability density function described by the Weibull distribution, with the purpose to generate random wind speeds for yearly time series to feed in the simulation. Anyway, in order to generate random numbers following a Weibull simulation with Excel, MatLab or almost any other software, it is necessary to perform a Weibull inversion.

The cumulative probability density function is generally defined as:

$$CDF(x) = \int_{-\infty}^{x} f(t)dt \tag{33}$$

Which for a Weibull distribution becomes:

$$Weibull\ CDF: F(x) = 1 - e^{-\left(\frac{x}{\eta}\right)^{\beta}} = R \tag{34}$$

Where R is a variable that has been defined as equal to F(x). From this, inverting and solving for x in terms of R we obtain:

$$x = \eta[-\ln(1-R)]^{\frac{1}{\beta}} \tag{35}$$

By generating uniformly distributed numbers R, for example with the Excel or Matlab *rand()* functions, and feeding them in such equation, it is possible to obtain random numbers following the specified Weibull distribution $We(\beta,\eta\ )$.

Anyway, generating random HAWS following such distribution is not enough to recreate a realistic time series. In fact, differences between consecutive hours are unrealistically irregular and high, and in the UC model they cause frequent switching on and off of thermal generators, which raises the costs and causes underestimation of the NPV. To recreate a more accurate time series, the sample of measured data has been used to study the HAWS differences between consecutive hours. The average variation between one hour and the following in the sample is of only ±1.0 m/s, but the variations have a wide range of amplitudes and in a few cases they have been even larger than ±15 m/s of difference. The histogram of the absolute values of such variations in the sample is shown in Figure 12, at intervals of 0.2 m/s, and it has been normalised to show relative probabilities for each HAWS class. For simplicity, a second histogram has been created, with HAWS classes of 0.5 m/s of width, and the relative probability for each class has been used as a discrete probability function. The synthetic HAWS time series are generated to follow the constraint that the hourly differences must follow the same discrete probability function.

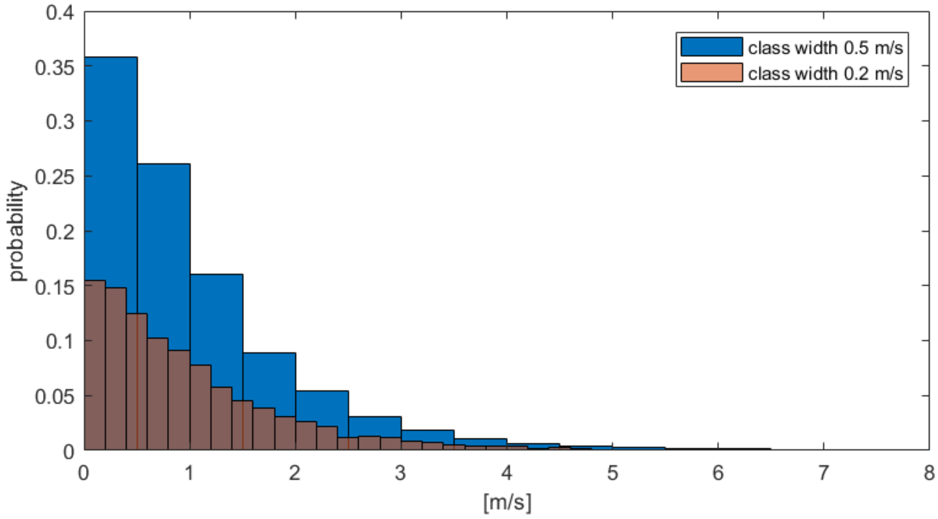


**FIGURE 12 – RELATIVE PROBABILITY FOR THE ABSOLUTE VALUE OF HAWS VARIATION OVER CONSECUTIVE HOURS**

As a verification criterion, the new distribution were fit with a Weibull distribution, whose shape and scale parametres are confronted with those of the sample year's distribution. If either of them differs of more than 5% from the sample parametres, the year is discarded. The resulting synthetic time series that are generated by this algorithm, respecting both the Weibull distribution and the probability distribution of the HAWS hourly differences, show a good similitude with the sample, as shown in Figure 13, and they appear to be well descriptive of the conditions that can verify over one year.

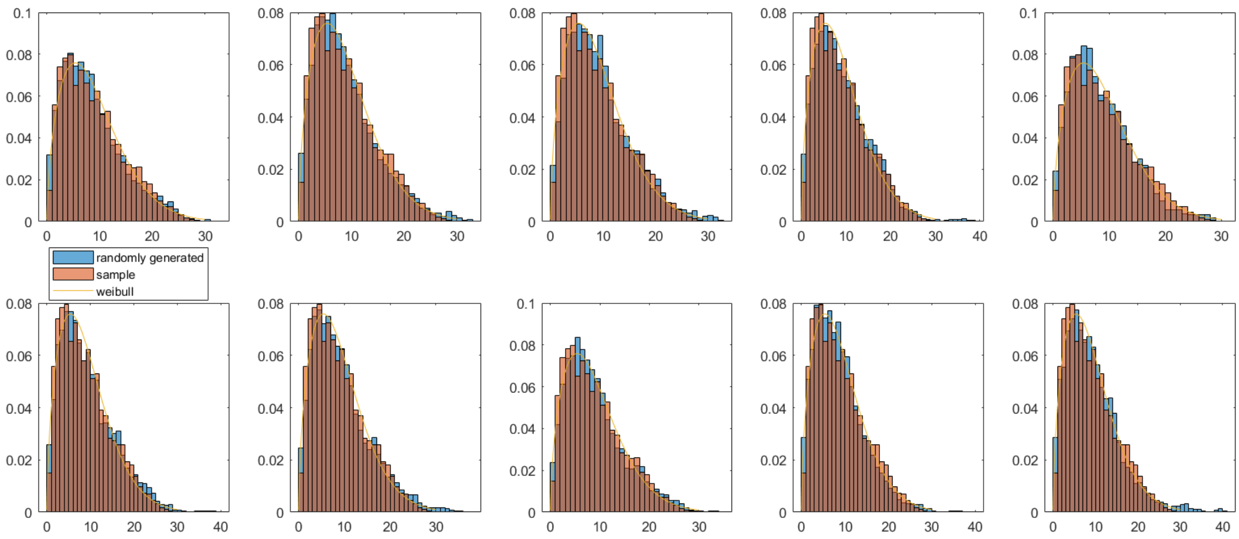


**FIGURE 13 – REPRESENTATION OF SOME OF THE RANDOMLY GENERATED YEARLY WIND SPEEDS (IN BLUE) NORMALISED HISTOGRAMS AGAINST THE SAMPLE YEAR (IN ORANGE)**

## 5.3. SOLAR IRRADIATION

The panel which has been chosen for the optimisation is LG NeON$_2$ [47], the company's best selling solar module and one of the most common in europe. It measures 1686x1016mm, and with its surface of 1.713 m$^2$ can provide a rated power of 335W with an efficiency of 19.6%. The assumption for panel configuration is the one of polar mounting, so with the panel facing south and with a tilt equal to the latitude of the location, to maximise overall yearly production. Inverter efficiency has been assumed as 97.5%.

**TABLE 3 – SUMMARY OF CHOSEN PV PANEL'S CHARACTERISTICS**

| | | |
|---|---|---|
| **NOCT** | [ °C ] | 45 ± 3 |
| **$P_{max}$** | [%/°C] | -0.37 |
| **$V_{oc}$** | [%/°C] | -0.27 |
| **$I_{sc}$** | [%/°C] | 0.03 |

The data for solar irradiation has been retrieved from SODA HelioClim-1 Database of Daily Solar Irradiance v4.0 (derived from satellite data) [48]. The data includes global horizontal irradiation and direct normal irradiation average values for each hour, for 11 years, 2005 to 2015. Starting from such data, a typical meteorological year TMY P50 has been assembled, with the methodology from [49] and [50]. The TMY is not very representative of hourly variations, due to cloudiness for example, but it is respectful of the overall energy balance over a period. More accurate and interesting stochastic and probabilistic modeling can be found in [51] and even more detailed stochastic methods are suggested in [52]. Anyway, because of the lack more accurate weather data, the TMY has been used in the model as it is, since any other method would have been based only on assumptions, and its increase (or decrease) in accuracy relative to reality could not have been quantified.

The efficiency of the panels has been related to the air temperature, with the parametres provided by the manufacturer and summarised in Table 3. The values for temperature are derived from the from monthly mean, minimum and maximum values from [53], and fitted with a sinusoidal function to obtain temperature values for each hour of the day, as shown in Table 4.

**TABLE 4 – AIR TEMPERATURES USED IN THE MODEL, IN AN HOUR/MONTH AXES SYSTEM**

| h | 1 | 2 | 3 | 4 | 5 | 6 | 7 | 8 | 9 | 10 | 11 | 12 |
|---|---|---|---|---|---|---|---|---|---|---|---|---|
| 0 | 13,5 | 13,4 | 13,5 | 14,2 | 15,5 | 17,3 | 18,8 | 19,5 | 19,6 | 18,3 | 16,2 | 14,5 |
| 1 | 13,5 | 13,4 | 13,6 | 14,3 | 15,6 | 17,4 | 18,8 | 19,5 | 19,7 | 18,3 | 16,3 | 14,5 |
| 2 | 13,8 | 13,7 | 13,8 | 14,6 | 15,9 | 17,6 | 19,1 | 19,8 | 20,0 | 18,6 | 16,5 | 14,8 |
| 3 | 14,3 | 14,2 | 14,3 | 15,0 | 16,3 | 18,1 | 19,6 | 20,3 | 20,4 | 19,1 | 17,0 | 15,3 |
| 4 | 14,9 | 14,7 | 14,9 | 15,6 | 16,9 | 18,6 | 20,1 | 20,9 | 21,0 | 19,7 | 17,6 | 15,8 |
| 5 | 15,6 | 15,4 | 15,6 | 16,3 | 17,6 | 19,2 | 20,8 | 21,6 | 21,7 | 20,4 | 18,3 | 16,5 |
| 6 | 16,3 | 16,1 | 16,4 | 17,0 | 18,3 | 19,9 | 21,5 | 22,3 | 22,4 | 21,1 | 19,1 | 17,2 |
| 7 | 17,0 | 16,8 | 17,2 | 17,7 | 19,0 | 20,6 | 22,2 | 23,0 | 23,1 | 21,8 | 19,9 | 17,9 |
| 8 | 17,7 | 17,5 | 17,9 | 18,4 | 19,7 | 21,2 | 22,9 | 23,7 | 23,8 | 22,5 | 20,6 | 18,6 |
| 9 | 18,3 | 18,0 | 18,5 | 19,0 | 20,3 | 21,7 | 23,4 | 24,3 | 24,4 | 23,1 | 21,2 | 19,1 |
| 10 | 18,8 | 18,5 | 19,0 | 19,4 | 20,7 | 22,2 | 23,9 | 24,8 | 24,8 | 23,6 | 21,7 | 19,6 |
| 11 | 19,1 | 18,8 | 19,2 | 19,7 | 21,0 | 22,4 | 24,2 | 25,1 | 25,1 | 23,9 | 21,9 | 19,9 |
| 12 | 19,2 | 18,9 | 19,4 | 19,8 | 21,1 | 22,5 | 24,3 | 25,2 | 25,2 | 24,0 | 22,1 | 20,0 |
| 13 | 19,1 | 18,8 | 19,2 | 19,7 | 21,0 | 22,4 | 24,2 | 25,1 | 25,1 | 23,9 | 21,9 | 19,9 |
| 14 | 18,8 | 18,5 | 19,0 | 19,4 | 20,7 | 22,2 | 23,9 | 24,8 | 24,8 | 23,6 | 21,7 | 19,6 |
| 15 | 18,3 | 18,0 | 18,5 | 19,0 | 20,3 | 21,7 | 23,4 | 24,3 | 24,4 | 23,1 | 21,2 | 19,1 |
| 16 | 17,7 | 17,5 | 17,9 | 18,4 | 19,7 | 21,2 | 22,9 | 23,7 | 23,8 | 22,5 | 20,6 | 18,6 |
| 17 | 17,0 | 16,8 | 17,2 | 17,7 | 19,0 | 20,6 | 22,2 | 23,0 | 23,1 | 21,8 | 19,9 | 17,9 |
| 18 | 16,3 | 16,1 | 16,4 | 17,0 | 18,3 | 19,9 | 21,5 | 22,3 | 22,4 | 21,1 | 19,1 | 17,2 |
| 19 | 15,6 | 15,4 | 15,6 | 16,3 | 17,6 | 19,2 | 20,8 | 21,6 | 21,7 | 20,4 | 18,3 | 16,5 |
| 20 | 14,9 | 14,7 | 14,9 | 15,6 | 16,9 | 18,6 | 20,1 | 20,9 | 21,0 | 19,7 | 17,6 | 15,8 |
| 21 | 14,3 | 14,2 | 14,3 | 15,0 | 16,3 | 18,1 | 19,6 | 20,3 | 20,4 | 19,1 | 17,0 | 15,3 |
| 22 | 13,8 | 13,7 | 13,8 | 14,6 | 15,9 | 17,6 | 19,1 | 19,8 | 20,0 | 18,6 | 16,5 | 14,8 |
| 23 | 13,5 | 13,4 | 13,6 | 14,3 | 15,6 | 17,4 | 18,8 | 19,5 | 19,7 | 18,3 | 16,3 | 14,5 |

Electric production in W/m$^2$ from the array of PV panels has been estimated using the HDKR model in [54]. Accoding to this model, the total useful radiation on the tilted surface is:

$$I_T = I_b + (I_{d,iso} + I_{d,cs} + I_{d,hz}) + I_r \tag{36}$$

Where $I_b$ is the beam or direct irradiance, $I_d$ is the diffuse irradiance, divided into its isotropic, circumsolar and horizon-brightening components, and $I_r$ is the radiation reflected from the ground. The isotropic component of the diffuse irradiance is received uniformly from the entire sky dome. Circumsolar diffuse originates from forward scattering of solar radiation; its name comes from the fact that it is concentrated in the part of the sky around the sun. Horizon brightening on the other hand is the sunlight scattering closer to the horizon, particularly noticeable in clear skies.

In the HDKR model, the sum of the components in equation (36) is rewritten as:

$$I_T = (I_b + I_d A_i) R_b + I_d (1 - A_i) \left(\frac{1 + cos\beta}{2}\right) \left[1 + f \ \sin^3\left(\frac{\beta}{2}\right)\right] + I \, \rho_g \left(\frac{1 - cos\beta}{2}\right) \tag{37}$$

Where $A_i$ is an anisotropy index, $R_b$ is the ratio of diffuse radiation on the tilted surface to that on the horizontal plane, $\beta$ is the tilt angle, $1 + \sin^3\left(\frac{\beta}{2}\right)$ is a correction factor to account for horizon brightening, $f$ is a modulation factor to in $I_{d,hz}$ to account for cloudiness, $I$ is the global horizontal irradiance (GHI) and $\rho_g$ is the ground reflectance.

In a first version of the model, also the panel degradation had been accounted for, as a 7.5% loss of production in the second year to account for discrepancy from rated conditions [55] and then 0.5% of degradation for the following years [56]. Anyway, because of the need to run again the UC model for every year, the PV panel degradation has been neglected to reduce the computational effort required by the model.

## 5.4. Geothermal and Energy Storage

Geothermal generators are modeled with the simplificative assumption that production is constant at any time, and equal to the nominal installed power. Anyway, frequency regulation is left to thermal groups, since geothermal generators have higher response time and are not suitable for that purpose. According to the analyses of EDA, a geothermal potential seems to exist in Faial up to 7.5 MW, but the experience of the company suggests that, as a rule of thumb, projects under 10 MW of power are under the financial viability threshold, as stated in a personal email exchange with an engineer from EDA. Nevertheless, some exceptions exist, as the main determinant is the success of the drilling phase and the availability of a reservoir of water as a heat transfer fluid. An example is the new geothermal plant in Terceira, which was inaugurated in autumn 2017 with a nominal power output of 3.5 MW [57].

As for energy storage, an in-depth research for the optimal storage means has been regarded as out of the boundaries of this work. The model is structured for a generic storage, and can be customised by changing the input data. The influence of storage's response time has been disregarded. For the Faial case study, the choice of the storage type has fallen on Li-Ion batteries, in particular on the Tesla PowerPack, which is one of the most competitive solutions on the market in terms of quality and cost. Li-Ion batteries are particularly suitable for this type of energy system, due to their multipurpose nature, not only as storage means but also for improving frequency quality. The efficiency of charge and discharge in this model is the same and equals to 92.5%; maximum Depth of Discharge (DoD) has been considered 100%, as reported by the manufacturer [58]. The battery is rated for 5000 cycles, so the expected lifetime has been assumed conservatively as 5 years, after which all storage system must be renovated.

BESS can actually be represented also by a fleet of plug-in hybrid and electric vehicles, in the so-called Vehicle-to-Grid (V2G) concept. As an example, considering that the base model of Tesla Model 3 has a battery pack of 50 kWh [59], a 10000 kWh nominal storage could be achieved with 200 cars, a reasonable amount to achieve in the near future. The regional government's strategic visions for 2020 include the promotion of electric mobility in the Azores, also as a mean to experiment with the impact of electric vehicles on the energy system [60]. In fact, in the Autonomous Region of the Azores, in 2016 an average of 22.64 light vehicle was sold every 1000 inhabitants, which translates in an average of 340 cars sold in Faial every year [61], a good part of which, with sufficient subsidies, could be electric.

## 5.5. Thermal generators

To cope with uncertainty in renewable energy generation, hybrid energy systems require from operators a certain amount of capacity committed in excess in respect to the forecasted load. Such excess capacity is called operating reserve, and can technically be divided into spinning and non-spinning reserve. Spinning reserve is represented by thermal generators connected to the systems, while non-spinning reserve is provided by fast-starting units such as batteries.

Spinning reserve requirements are usually imposed by the system operator; in the case of EDA, they are usually related with the wind installed capacity. Currently, in Terceira island the strategy followed by EDA is the following [22]:

$$SR_t = \begin{cases} 50\% \cdot x_1 & if\ HAWS_t > 15\ m/s \\ P_t^{wind} & if\ HAWS_t \leq 15\ m/s \end{cases} \quad (38)$$

Such spinning reserve strategy is mostly based on the operator's direct experience about network stability issues caused by high wind penetration. It is reasonable to assume that the same strategy can be adopted in other microgrids system, because of the similar characteristics, and in particular in Faial, the case study adopted in this work.

Thermal generators are modeled individually, rather than aggregating them in a single function, by using the data of the current generators in Faial presented previously in Table 2. As more extensively mentioned in section 3.3, the code used for UD+EC problem has been retrieved from [32], and it has been edited for interfacing with the rest of the code. Their behaviour has been regulated through an economic dispatch model which takes into account their operating cost and their startup cost, while their shutdown cost has been assumed as negligible again due to the small size of the generators. The quadratic formula for operating costs, expressed in equation (17) in section 3.3, uses three coefficients usually provided by the manufacturer of the generators. Because of the difficulty of obtaining these coefficients for the generators in Faial, the coefficients for the generators in Terceira have been taken from [22] and rescaled assuming that all three of them vary linearly with the generator rated power, as illustrated in Figure 14. This assumption seems reasonable when looking the trend of the costs over the output power, shown in Figure 15.

Anyway, to achieve higher computational speed, a further simplification has been adopted in the optimisation phase only, by replacing the quadrating operation cost formula of the generators with a linear equation, shown in Figure 15 and reported in equation (39):

$$Cost_{t,i} = 57.68 \cdot \left(P_{MWt,i}^{therm} - 1\right) + 30.21 \quad (39)$$

**TABLE 5 – SUMMARY OF THE HOURLY COST PARAMETRES FOR THE THERMAL GENERATORS IN FAIAL**

| | SIZE [MW] | a [€] | b [€/MW] | c [€/MW$^2$] | StUp [€] |
|---|---|---|---|---|---|
| **KRUPP** | 2 | -15.55 | 43.87 | 1.889 | 43.33 |
| **SULZER** | 3 | -3.27 | 43.13 | 1.783 | 52.92 |
| **CAT** | 3.7 | 5.33 | 42.61 | 1.709 | 60.87 |
| **TERCEIRA1** | 5.9 | 32.35 | 40.99 | 1.476 | 105.25 |
| **TERCEIRA2** | 12 | 107.27 | 36.49 | 0.830 | 398.45 |

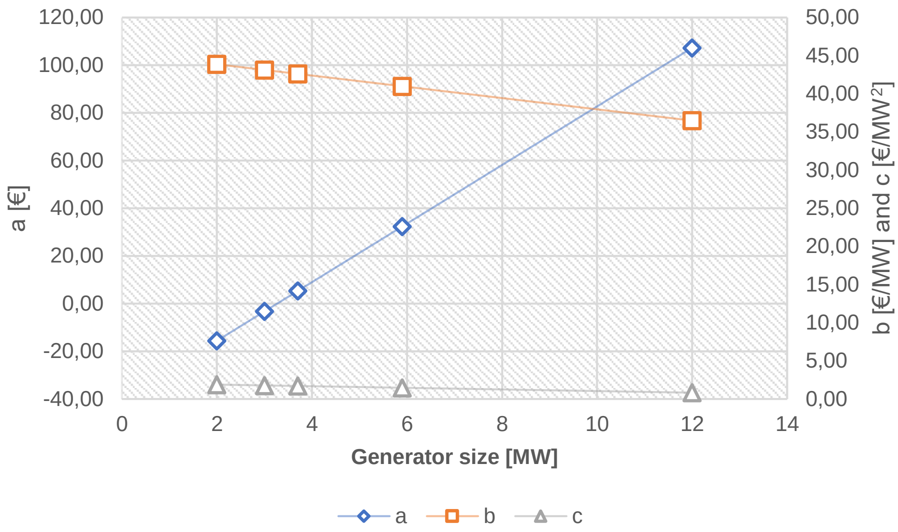


**FIGURE 14 – VARIATION OF PARAMETRES FOR QUADRATIC PROGRAMMING ED WITH GENERATOR SIZE**

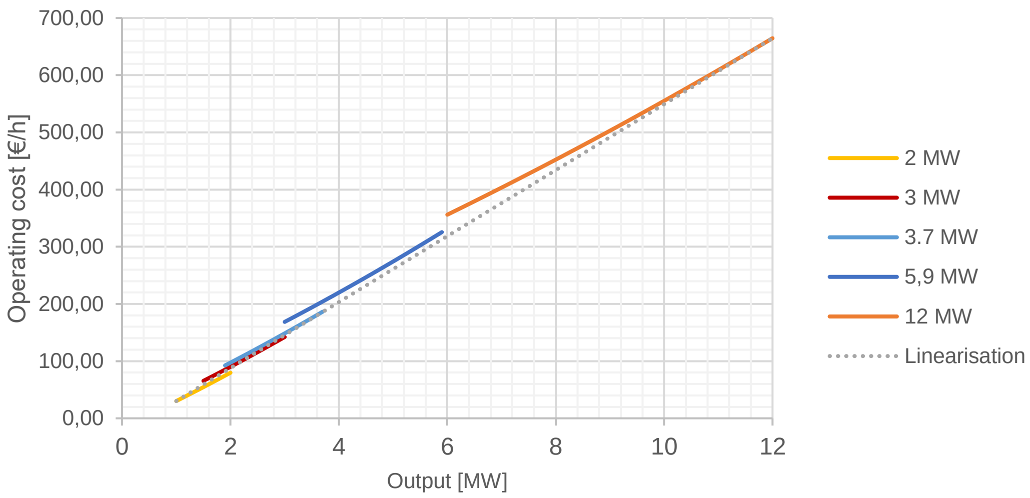


**FIGURE 15 – OPERATING COST IN €/H AS A FUNCTION OF THE OUTPUT POWER OF EACH GENERATOR**

As for the variation of startup costs with the size of the generator, it has been assumed that an exponential curve could be a reasonable scaling for generators of smaller size, as shown in Figure 16. Again, the data for startup costs for thermal units in Terceira comes from [22].

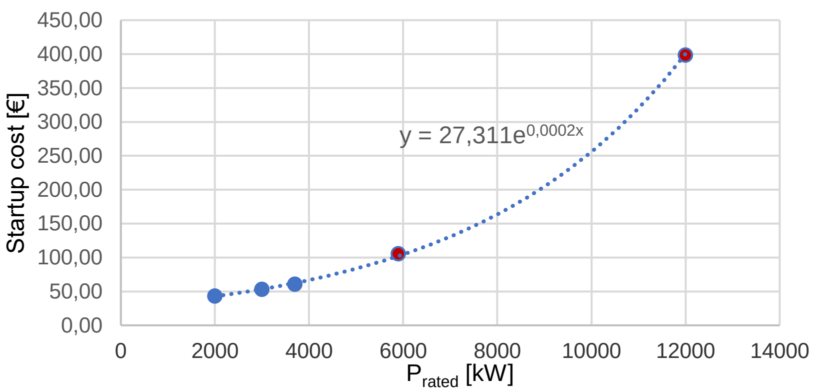


**FIGURE 16 – VARIATION OF STARTUP COST WITH GENERATOR RATED POWER**

For what concerns the operational constraints, the minimum power that a generator can supply has been set as 50% of its rated power. Ramp up and down constraints have been regarded as negligible, as well as the minimum downtime and uptime. Such assumption can be justified considering the small size of the generators in the microgrid, which allows a more flexible use of the gensets.

As for pollutant emissions, they have been computed to be onverted into a cost in the environomical optimisation, using a carbon tax calculated on the yearly tons of $CO_2$ emitted. The fuel consumption has been assumed to be constant, with the value of 177 $g_{fuel}$/kWh provided by the manufacturer for CAT 8C M32C [62] and assumed to be the same for the other engines. Also, from the same manufacturer spreadsheet, the consumption appears to remain roughly unchanged regardless if the engine is used at 50% or 100%. Using a LHV of 40.19 MJ/kg for HFO and a carbon emission factor of 0.0202 $kg_C$/ MJ, the resulting $CO_2$ generation has been estimated as 2.977 $kg_{CO2}/kg_{fuel}$ [63].

## 5.6. Economic input data

This paragraph collects all the assumptions that have been used as inputs of the economic model for the calculation of the NPV. A research has been performed to find reasonable and up-to-date values for investment and operation cost for all the technologies used as decision variables in the model. As well as that, the financial position of EDA has been investigated to use accurate and realistic data regarding interest rate, cost of capital and all other economic parametres influencing the project.

As summarised in Table 6, the interest rate for EDA has experienced a decreasing trend in the last decade, thanks to the help of Investment European Bank subsidies. In absence of more recent data, the 2016 value of $r = 1.3\%$ has been assumed to be still valid [41].

**Table 6 – Evolution of interest rates for EDA in years 2008 - 2016**

| AVERAGE COST OF DEBT | |
|---|---|
| **2008** | 5,00% |
| **2009** | 2,90% |
| **2010** | 2,60% |
| **2011** | 3,50% |
| **2012** | 4,80% |
| **2013** | 3,70% |
| **2014** | 3,00% |
| **2015** | 2,30% |
| **2016** | 1,30% |

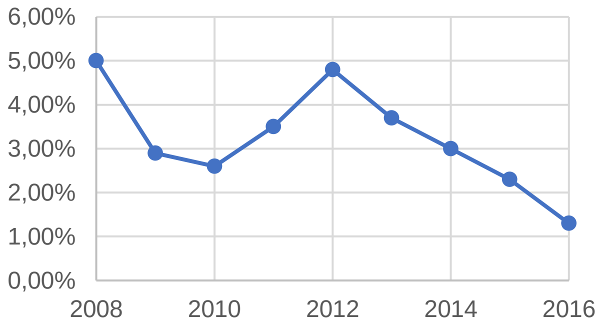


New investments of the utility have been assumed to be financed with 40% equity and 60% debt, which is a reasonable rule-of-thumb assumption. Cost of equity $k_e$ has been assumed at 12% to be conservative, and tax rate at 25%. As in equation (40), the resulting Weighted Average Cost of Capital (WACC) is 5.39%.

$$WACC = \frac{Debt}{Debt + Equity} \cdot r\,(1 - tax) + \frac{Equity}{Debt + Equity} \cdot k_e = 5.39\% \qquad (40)$$

Project insurances for full cover material damage has been assumed to account for 0.4% of CAPEX, and Advance Loss of Profit (ALOP) for delayed completion coverage or delay in start-up (DSU) is set as 0.6% of the EBITDA. Debt is assumed to have a 10 year horizon, while depreciation is calculated over 5 years, assuming that since the project involves renewable energy the company is allowed to take advantage of this incentive measure. As a matter of fact, accelerated depreciation can be fully taken advantage of only whitin the limits of the project owner's tax burden, which in this case is assumed to be high enough to allow EDA to claim the entire incentive. The NPV of the project is evaluated over 20 years, with a residual value of 10% at the end of the period to accout for materials and components that can be reused.

Cash flows also account for inflation with a growth factor of 1.4% [64].

Investment and O&M costs for the four involved technologies are summarised in Table 7.

TABLE 7 – SUMMARY OF CAPEX AND OPEX COSTS FOR THE TECHNOLOGIES OF THE DECISION VARIABLES

| | CAPEX [€/kW] | OPEX [€/kW/y] |
|---|---|---|
| **WIND** | 1530 | 42 |
| **PHOTOVOLTAIC** | 1000-2500 | 30 |
| **GEOTHERMAL** | 4000 | 90 |
| **STORAGE** | 350 €/kWh | 15 €/kWh/y |

As previously mentioned in section 4.1, the average retail price of electricity in Faial is 162.85 €/MWh.

The CAPEX for wind turbines has been extrapolated from the project of Salão in Faial, which totalled up to 6.5 M€ of investment, for an average of 1530 €/kW. O&M costs sum up to 42 €/kW/y according to [65], considering both planned maintenance (19 €/kW/y) and unplanned servicing (23 €/kW/y).

As for the photovoltaic system, projects globally installed in 2017 presented a cost between around 850 €/kW (5th percentile) and 2800€/kW (95th percentile) [66]. Considering that costs in EU tend to be more on the lower side, while costs in the US are higher, it is reasonable and conservative to assume a price around 1200 €/kW. However, in order to keep into account the variation of the cost with the size of the plant, this work benefits from a model previously developed for a project in Haiti owned by Colombian utility Celsia Energia, company in the Grupo Argos. The cost projections of Celsia are shown in Figure 17.

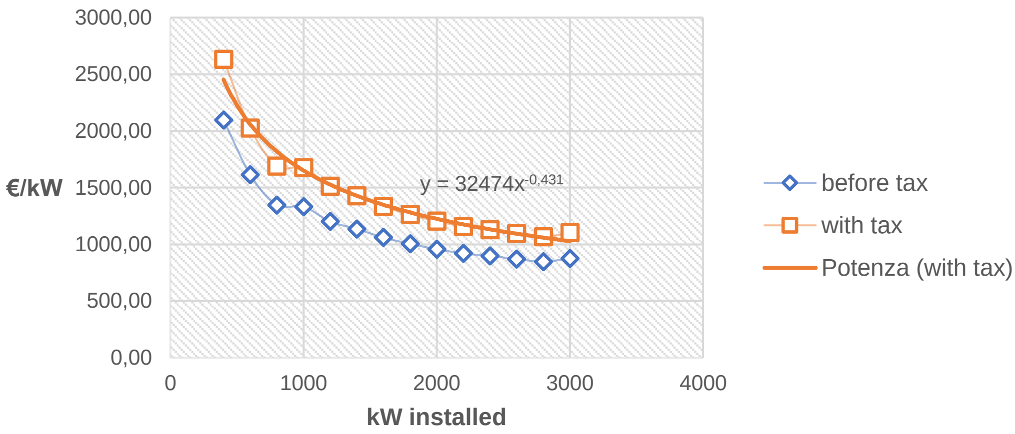


FIGURE 17 – COST PROJECTIONS FOR PV PANELS

To allow for continuity, the data have been fitted as a power function of the installed capacity $x_2$ as follows:

$$PV_{CAPEX} = \begin{cases} 2500 \dfrac{€}{kW} & if\ x_2 < 410kW \\ 32474 \cdot x_2^{-0.431} & if\ x_2 \geq 410\ kW \end{cases} \tag{41}$$

As for PV's O&M, the NREL baseline for utility-scale projecs is 14.5€/kW/y, but costs can vary between 8.50€/kW/y to 30€/kW/y [67] . Considering the difference in the location and in the energy market prices, the value of 30€/kW/y has been used as a conservative assumption.

The 10 MW geothermal plant of Pico Vermelho in São Miguel was constructed with a 34.4 M€ investment, which means an average of 3440 €/kW, value that has been assumed valid also for new projects in the Azores. The opex cost has been set conservatively at 90 €/kW/y following the considerations in [68].

Regarding Li-Ion batteries, the most competitive solution on the market in terms of batteries is the Tesla Powerpack, whose price is around 350€/kWh [69]. O&M for this type of battery is usually quite low, around 15 €/kWh/y of capacity installed [70].

The cost for the inverter has been conservatively assumed at 150 €/kW of PV installed [71], which is between the current prices for commercial and for utility-scale projects, because virtually the installed PV power could be obtained also with residential projects around the island. New transmission lines have been assumed at 65€/kW of the inverter's installed power. Investment for cables, lightning protection and all auxiliary systems is assumed at 10% of the cost of the inverter. O&M for inverters, transformers, electric lines and auxiliary devices is assumed at an yearly 5% of the CAPEX.

# 6. RESULTS

As explained in section 3.2, the optimisation model maximises the NPV as objective function. Anyway, in order to keep into account the current status of the energy system in Faial, the objective function has been preliminarily ran using as inputs the renewable capacity already installed in the island, together with the thermal generators. The resulting NPV of the current situation is the parametre used for comparison during the simulations. In order to do that, the objective function has been defined as the difference of the NPV of the new configuration and the benchmark NPV of the current configuration. In this way, the objective function yields positive results only when a proposed solution turns out to be more economically convenient than the present energy system. The benchmark NPVs have been calculated in three sub-scenarios of the current configuration: a basic scenario without any carbon tax, a scenario with a carbon tax of 6 €/ton, which is the current one in Portugal [72], and a third scenario with a doubled carbon tax 12 €/ton. Also, since EDA deems geothermal projects below 10 MW not feasible, for each of the three scenarios two cases have been included, with and without geothermal in the decision variables, for a total of six different scenarios.

## 6.1. BASE CASES

The benchmark NPVs used as references for the other simulated scenarios are also referred as base cases in this work. They represent the current energy system in Faial and its actualised value over the next 20 years, summarised in Figure 18. It is not clear whether the Autonomous Region of the Azores has a carbon tax or not. In continental Portugal it amounts to 6 €/ton$_{CO2}$; as a base for comparison, other European countries have rates between 4 and 30 €/ton$_{CO2}$ [72]. As a consequence, it has been deemed interesting to study a situation where no carbon tax is present, a situation with the above mentioned 6 €/ton$_{CO2}$ carbon tax, and an hypothetical situation in which such carbon tax is doubled, amounting to 12 €/ton$_{CO2}$, in order evaluate how such policies influence the optimal design of the HES.

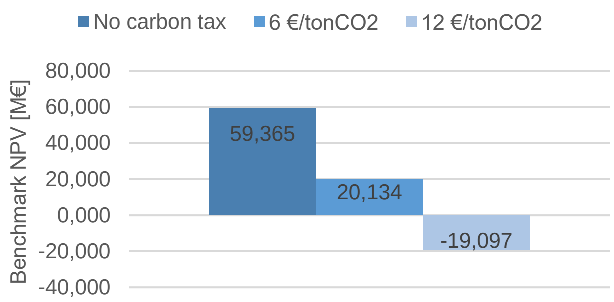


**FIGURE 18 – BENCHMARK NPV OF THE THREE BASE CASES, FOR CALCULATION OF COMPARED NPV**

Regardless of the presence of a carbon tax, which changes only the monetary value, the REF of the base case using the model of this thesis with the data of 2017 is 24.8%. This value, produced by only the Salão wind park, is not far from EDA's forecast of 20% estimated when the wind park was built, but at the same time it is significantly different from the measured 9.7%. The model actually gives quite optimistic forecasts, because of its simplificative assumptions, for example the facts that wind speed is considered to be the same on all turbines, that wake effects are neglected, that down-time and maintenance are not accounted for, and that the influence of wind direction is neglected.

## 6.2. THE SCENARIOS

The optimal configurations of the system are represented in Table 8 and reported in detail in Annex A , in the six scenarios obtained by the combination of the different carbon tax possibilities and of the inclusion or exclusion of geothermal technology. The plots show the optimal components' size against the variation of the minimum REF constraint, and keeping a minimum EIR constraint of 99%. The considerations that can be done are the following:

- Geothermal tends to enter the system before PV thanks to its higher productivity throughout the year. In fact, from weather data of Faial it appears that an average of 185 days per year are rainy, reducing drastically the amount of solar resource that can be exploited [73]. Geothermal optimal capacities are reasonable for a project in Faial, in case a good reservoir with the adequate presence of fluid is found.
- Wind capacity tends not to increase from the current installed capacity, which is already quite high. At first sight this might appear paradoxal, considering the productivity of such technology, but the cause is in the definition of Spinning Reserve as a function of the installed wind capacity. Installing more wind turbines leads to higher SR requirements, which will force higher RES curtailment; as a result, increasing wind capacity actually conflicts with the increasing RES constraints.
- When a higher Renewable Energy Fraction is forced, the energy storage need in the system grows exponentially. Anyway, considering that the Li-Ion BESS in the Graciosa project has a capacity of 3.2 MWh [29], and considering the proportion between the energy system of Graciosa and that of Faial, it is unrealistic to think of a BESS for Faial larger than 9÷12 MWh. The reason for the large need for storage highlighted by the model is again in the impossibility of increasing wind penetration.
- In presence of a carbon tax, even when the minimum constraint for REF is low, for example 20% or 25%, the model converges to an optimum point with a REF higher than the constraint, reaching up to 65.2% in the case with geothermal and with a 6 €/ton tax. This shows that carbon taxes can incentivate to the installation of renewables, which become more economically convenient than thermal generators.

  Anyway, since a large fraction of the energy of the island still needs to be produced with fuel, this measure also raises the costs resulting in a significantly lower NPV of the project, making it less feasible for the company. This is an interesting example of how carbon taxes should be used in combination with other policies, otherwise they might create unavoidable losses for utilities reducing their possibilities for new investments.

Furthermore, considering the available surface in Faial, the optimal configurations appear to have unreasonable capacities of PV to install, when geothermal is excluded from the decision variables. To fine-tune the results to more realistic solutions, a second round of simulation has been performed with a maximum limit of 1.5 MW of PV rated power. Such limitation has been chosen after considering the two EDA projects for PV plants, of 1 MW in Graciosa [29] and 600 kW in Santa Maria [3]. Results are presented in Table 9 and again, more in detail in Annex A .

With this limit on PV, if geothermal is constrained the same thresholds of REF can be obtained only with an even higher storage capacity, which is so unrealistically high that is not even visible in the plot. Anyway, when a constraint on the maximum storage capacity is imposed, the optimisation model can not find any solutions with REF higher than 30%. This is again due to how SR is defined, which leads to the conclusion that islanded systems with high RES penetration need more accurate and dynamic strategies for spinning reserve management, which should also involve BESS as non-spinning reserve.

As for the NPVs of the optimised system when the minimum REF constraint is varied, a more immediate representation for comparison between the six scenarios is reported in Figure 19 and Figure 20. It can be immediately noticed that scenarios using geothermal energy tend to reach higher NPVs, often greater than zero. The drop of some NPVs in Figure 20 is the consequence of the cap imposed on PV: the limitation of its installed power makes a larger storage capacity necessary to reach the minimum REF constraint when other RES capacity can not be increased, which makes costs rise and the NPV fall.

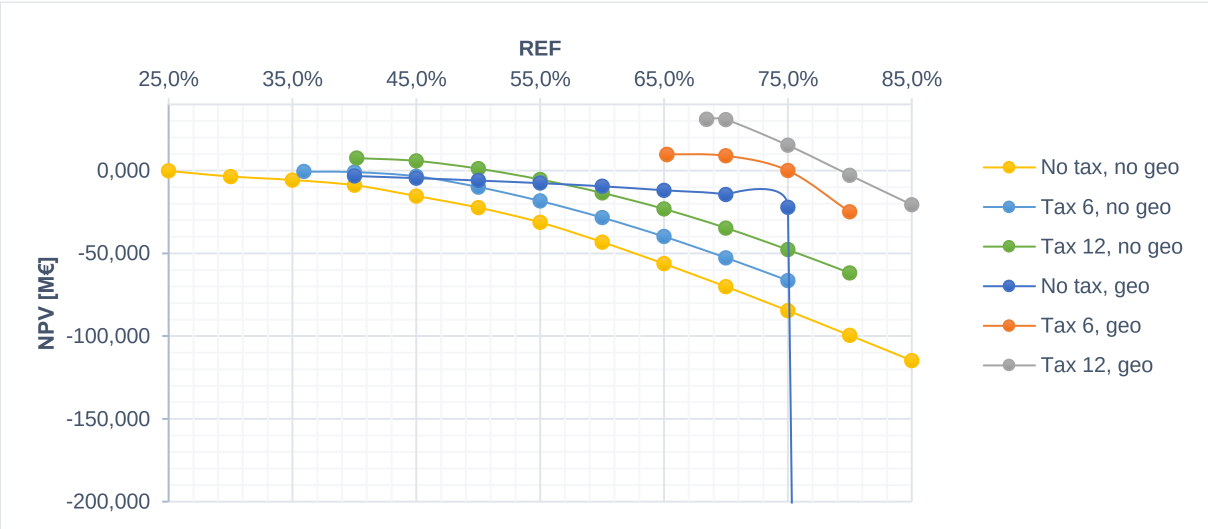


FIGURE 19 – NPV OF THE OPTIMAL DESIGNS, WITH AND WITHOUT GEOTHERMAL, VARYING REF AND CARBON TAX

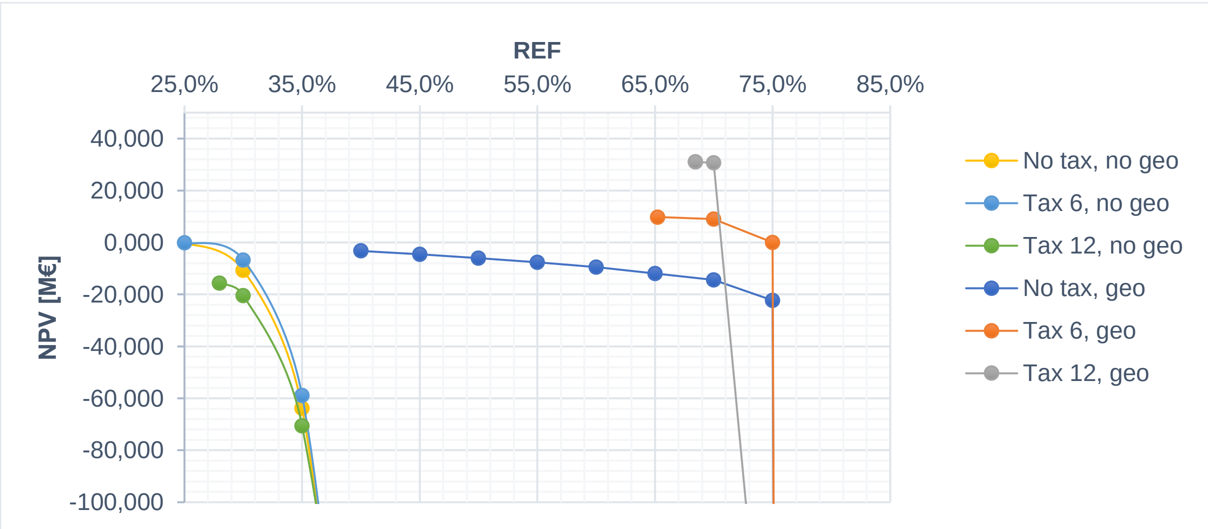


FIGURE 20 – NPV OF THE OPTIMAL DESIGNS WITH PV LIMITATION AT 1.5 MW

TABLE 8 – SIMULATION RESULTS. TOP LINE IS WITH GEOTHERMAL, WHILE BOTTOM LINE IS WITHOUT GEOTHERMAL

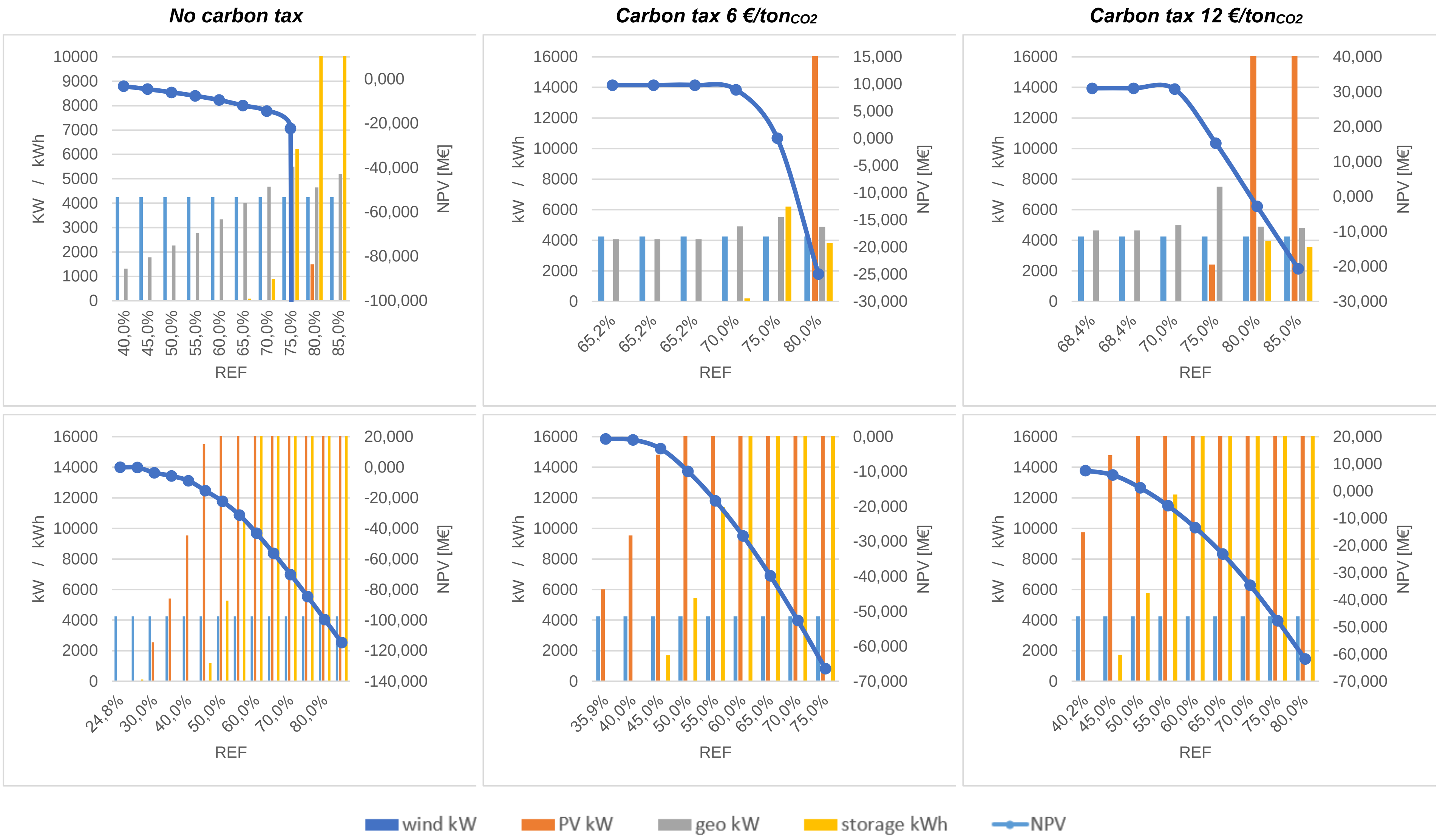

TABLE 9 – SIMULATION RESULTS WITH LIMITATION OF PV CAPACITY AT 1.5 MW

| *No carbon tax* | *Carbon tax 6 €/ton$_{CO2}$* | *Carbon tax 12 €/ton$_{CO2}$* |
| --- | --- | --- |

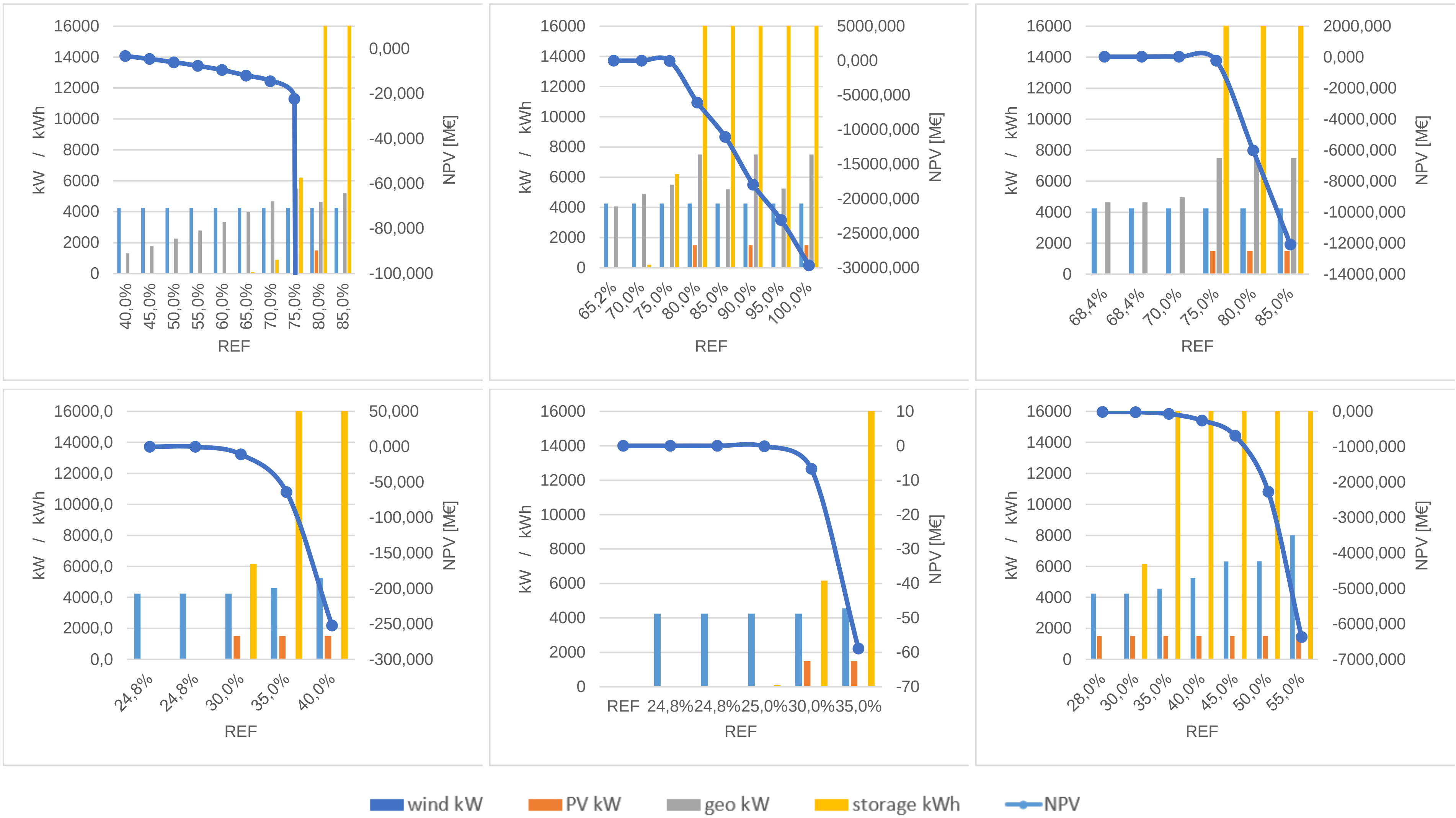

## 6.3. Sensitivity analysis and Monte Carlo simulations

Amongst all these scenarios presented in Table 8 and Table 9, the one which reaches the highest REF at the same time featuring the most realistically feasible configuration is the hybrid wind/geothermal/BESS energy system designed for a REF of 75%. The system requires a total investment of 28.85 M€, of which roughly 78% only for the geothermal plant, and has a NPV of only 43'000€ when compared to the current system configuration in Faial, considering a scenario with the current Portuguese carbon tax of 6 €/ton$_{CO2}$. From the optimisation, a system designed for REF 70% appears to have a definitely higher NPV, roughly 9.8 M€ as shown in Figure 21, but the design for 75% has been chosen because is more ambitious in terms of renewable penetration, is more interesting to study due to its higher storage capacity, and still presents a positive NPV, thus representing a situation in which the company is reaching the break-even point of the investment.

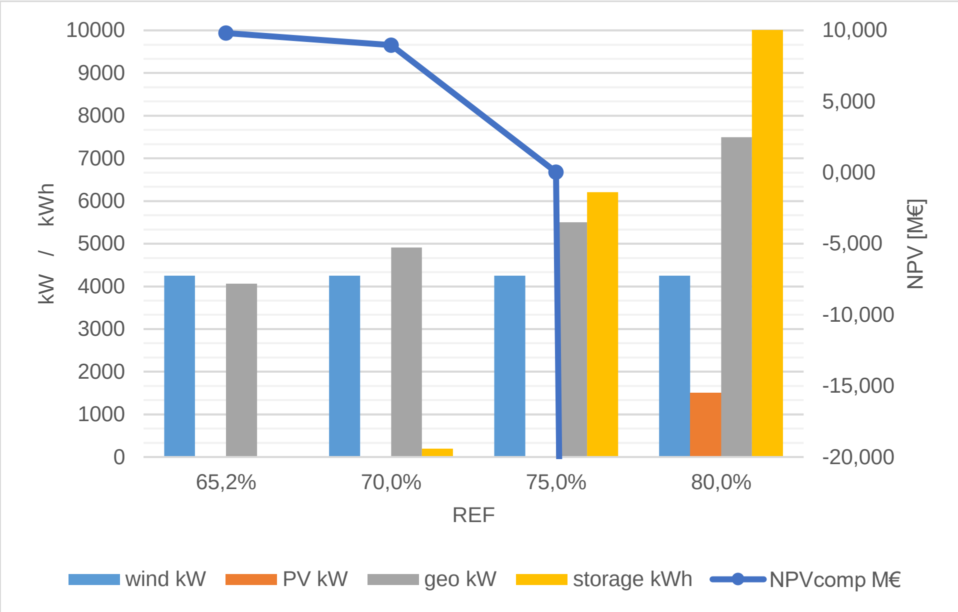


Figure 21 – Detail of the optimisation results with limit on PV and carbon tax 6 €/ton$_{CO2}$

The installed capacities of the HES are shown in Table 10. This HES configuration has been studied more in detail to analyse its energy and economic behaviour when there is a variation in the conditions used for the optimisation, such as the electricity price, the debt interest rate, the wind speeds over the year, or the uncertainty in the load curves.

Table 10 – Installed capacity in the design chosen for sensitivity analysis

| | |
|---|---|
| **WIND** | 4250 kW |
| **GEOTHERMAL** | 5504 kW |
| **STORAGE** | 6208 kWh |

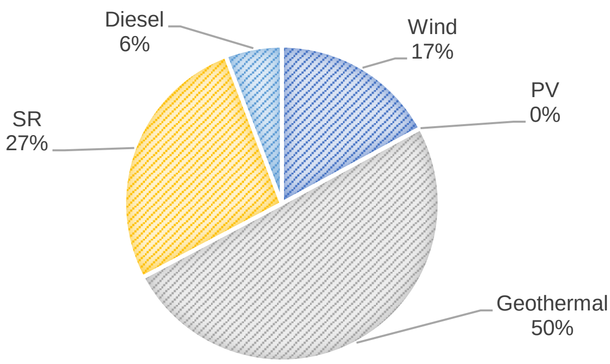


**FIGURE 22 – BREAKDOWN OF ENERGY PRODUCTION FROM THE SELECTED DESIGN**

As visible in Figure 22, with the chosen system design 50% of the energy production comes just from the geothermal plant, while wind is responsible for 17% of the production. Such percentages have been calculated assuming that all the curtailed and dissipated energy comes from renewables only, in proportion with their relative production shares. To be true, part of the energy dissipated in the battery charge and discharge comes from thermal generators too, which leads to wind and geothermal shares in the breakdown summing up to a lower amount than the "nominal" 70%. Due to the oversizing of the components, the energy that is curtailed every year is a very large amount, summing up to 53% of the total yearly demand.

With this system configuration, the usage of thermal generators already present in Faial has been determined with the UC+ED model, resulting in what is shown in Figure 23. The system relies mostly on only two of the six generators, G4 and G5, while G3 provides a backup when the gap between load and RES production is particularly high. The three Caterpillar/MAK generators, with the largest rated power and higher operational costs, are not used in ordinary conditions, and can be either kept as a backup when the three main gensets are under maintenance, or decommissioned. Thermal generators provide 33% of the total energy generation, of which around 51% is produced through the smaller generator, the 2MW Krupp.

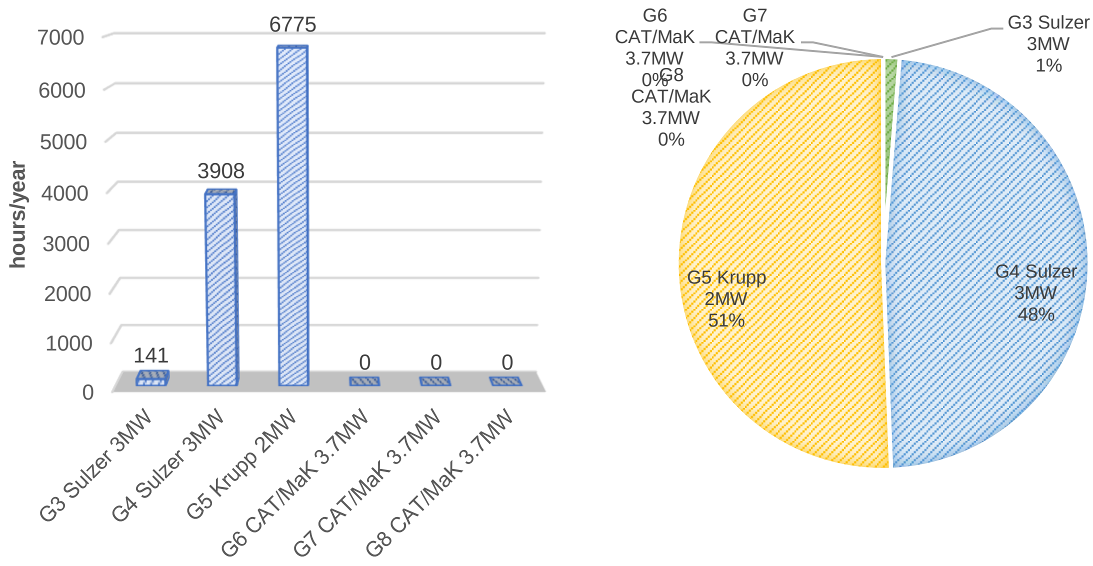


**Figure 23 – Hours of usage of thermal engines in the chosen design, and breakdown of corresponding energy production**

The possibility of decommissioning the less used generators has also been recognised by EDA, because of the old age of some engines, of environmental constraints and of their low utilisation, in some cases less than 500 h/year [3].

The results have been validated with an optimisation model built in HOMER software. As shown in Figure 24, the solution which is closer to the design determined with the MatLab model is not very different from the one analysed in this chapter. The design, featuring a 9 MWh Li-Ion BESS, introduces only 2MW of geothermal power in order to reduce the excess electricity to be wasted. This system can reach a REF up to 63.1%, according to the software.

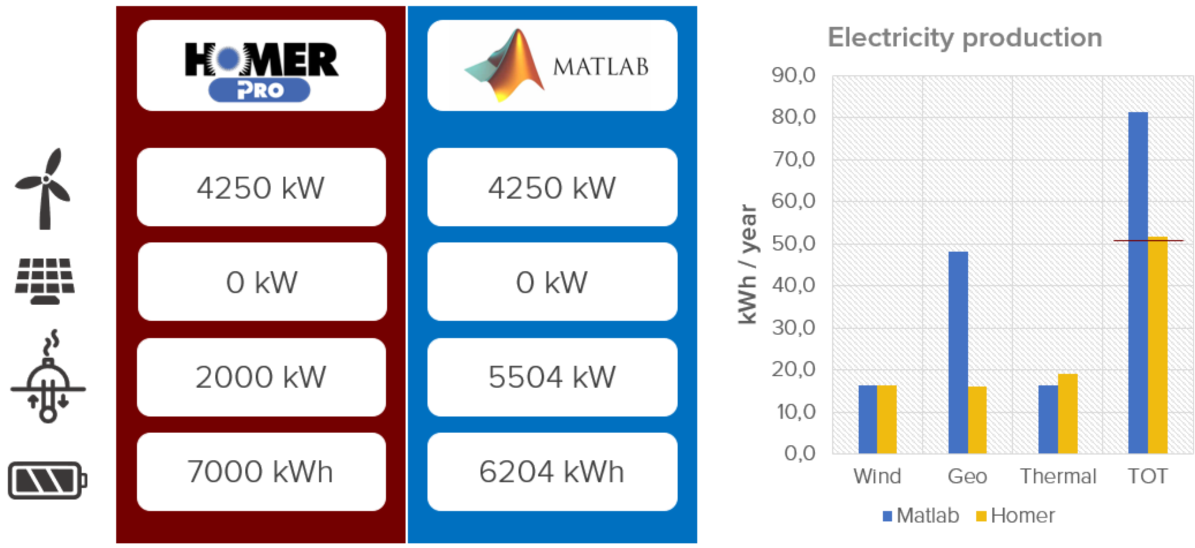


**Figure 24 – Comparison of the results of the optimisation with one of the optimal designs from HOMER**

A sensitivity analysis of the NPV has been performed by varying the electricity retail price, and has resulted, as expected, in a linear trend, as shown in Figure 25. The base electricity price, plotted in red, is 162.85 €/MWh as explained in sections 4.1 and 5.6. One of the measures that can be taken by EDA to increase the secutiry of the project feasibility is to increase slightly the average electricity price, for example to around 180 €/MWh, with the results shown later in this chapter.

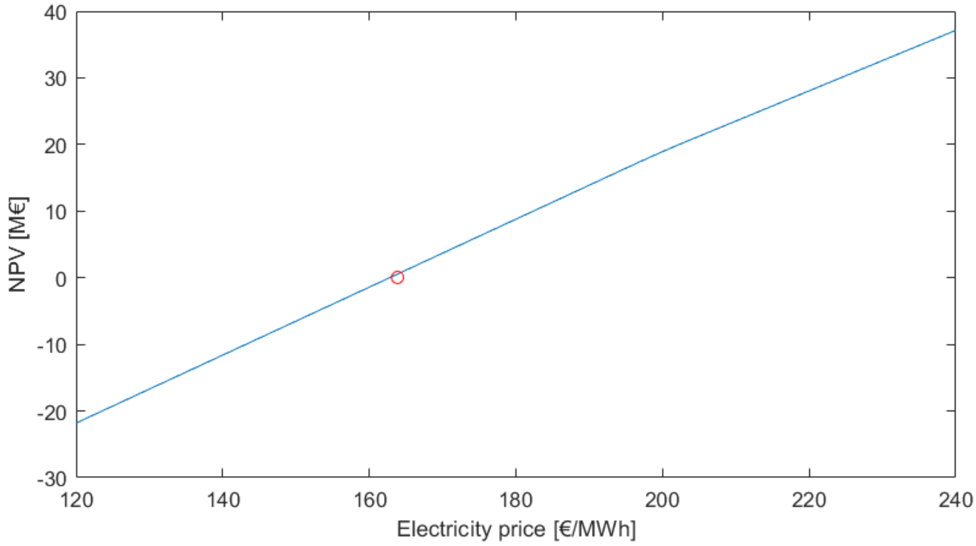


**FIGURE 25 – SENSITIVITY ANALYSIS ON ELECTRICITY RETAIL PRICE**

As expected, also the debt's interest rate has a significant impact on the project NPV, influencing linearly the WACC which is used to discount all the future cash flows. When electricity price is kept constant, the reduction of NPV when a higher interest is present is shown in Figure 26.

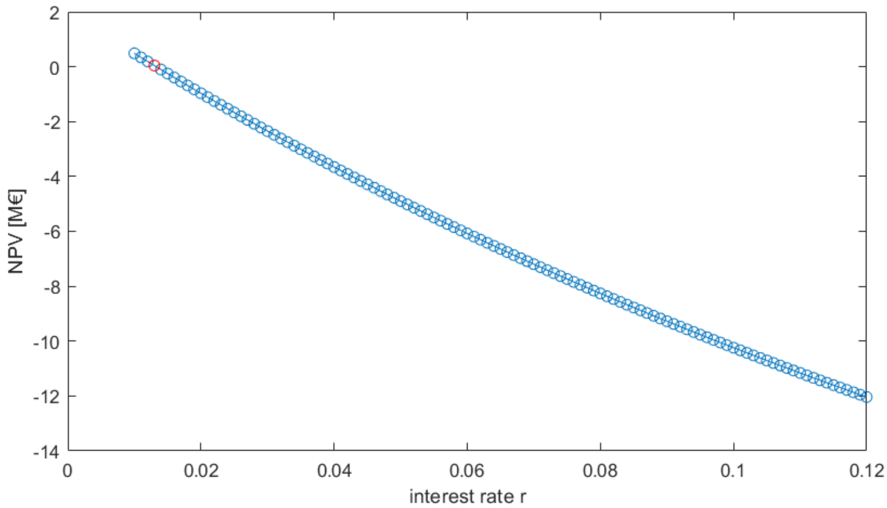


**FIGURE 26 – SENSITIVITY ANALYSIS ON INTEREST RATE OVER DEBT WITH BASE ELECTRICITY PRICE**

Another factor which is necessary to study is the impact of uncertainty in the stochastic variables. To this purpose, Monte Carlo simulations have been performed on 2000 different randomly generated time series, both for wind speed and for electric power demand, while the other variables such as the electricity price of 162.85 €/MWh are kept constant.

The results of Monte Carlo simulation with HAWS synthetic time series are shown in  Figure 27, with the base electricity price and with the price of 175 €/MWh. Depending on wind speed throughout the year, the NPV can vary even of few million euros, and with the base price has a probability of 52.5% of being lower than zero. With a sufficient increase in retail price, for example to 175 €/MWh, such probability decreases to values close to zero.

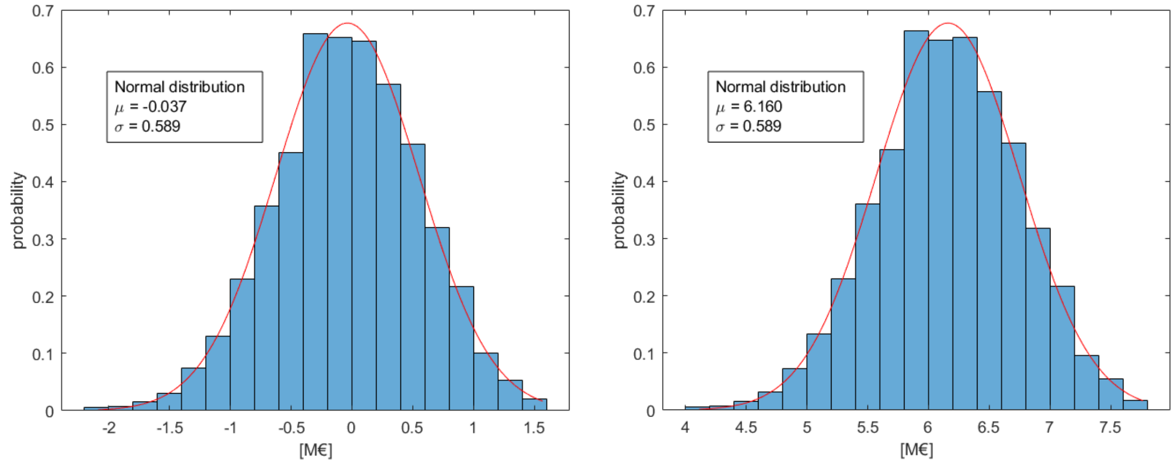


**FIGURE 27 – MONTE CARLO SIMULATIONS OF PROJECT NPV DEPENDING ON WIND CONDITIONS, WITH ELECTRICITY RETAIL PRICE OF 162.85 €/MWH AND 175 €/MWH**

In both simulations the EIR has always reached 100%, demonstrating a good flexibility of the system in adapting to variations in the operating conditions. The average REF of the analysed scenarios is 74.6%, close to the “rated” 75%, although it is important to remember that the model tend to overestimate the REF in respect to the actual production.

A Monte Carlo simulation with stochastic loads has been performed as well, and its result is presented in Figure 28, where it is possible to observe both graphically and comparing the standard deviations how the electric load has lower influence on the NPV than wind conditions. The probability that NPV is lower than zero because of variations in the electric demand profile is 26.2%. Also in this simulation an EIR of 100% has always been reached.

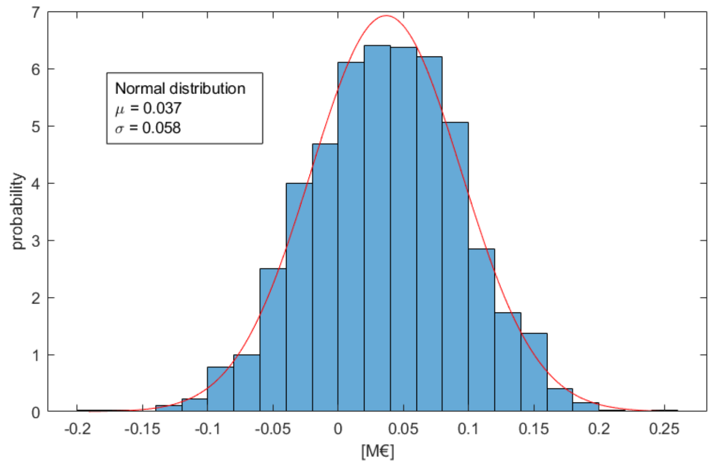


**FIGURE 28 – MONTE CARLO SIMULATION OF PROJECT NPV WITH LOAD CURVE UNCERTAINTY**

# 7. CONCLUSIONS

Several conclusions can be taken from the results of the model proposed in this work, some fostering an optimistic perspective on the deployment of renewables in the Azores and in microgrids in general, and some highlighting the need for analyses based on more accurate data to develop a successful project.

- The model elaborated in this thesis proved to be a flexible tool with a good level of accuracy in determining the optimal configuration of a hybrid renewable energy system and its financial viability, although overestimating the renewable production.
- The project in the examined case study appears to be proportioned to EDA's financial possibilities and to be coherent with the framework of investments of the company, totalising an initial investment of 28.85 M€ for a NPV of only 43'000€ when compared to the current system configuration. Moreover, the NPV can rise to roughly 6 M€ with an adjustment of the electricity retail price of around 10 €/MWh. Nevertheless, the presence of subsidies from Portuguese government and European Union is fundamental to support financially new projects of this type and scale.
- Wind energy appears to have already reached its saturation capacity in the island of Faial, satisfying around one fifth of the demand. On the other side, photovoltaic technology does not represent a strategic asset due to the low productivity and the land availability constraints that put it in a less preferential position compared to BESS or geothermal. All the designs in which PV is featured appear to have a negative NPV, apart from a design in the 12 €/tax scenario which requires 7.5 MW of storage, 2.4 MW of PV and no BESS, which is probably beyond the technical limits of viability.
- Energy storage technology has a fundamental role in island-mode microgrids with high penetration of renewables. The introduction of BESS alone offers the possibility to increase the renewable energy fraction in a HES, in a proportion increasing with the RES capacity in the system. In the case of Faial for example, the addition of a 6.2 MWh BESS (the size of the BESS in the studied optimal solution) to the current system raises the estimated REF to 27.0% only, against the initial 24.8%. If a geothermal plant of 5.5 MW is present, instead, the presence of the same BESS makes a difference from 71.5% to 75.0%, which means a 60% higher impact from the previous case. The benefits derived from storage can become even higher in presence of RES with a more irregular production such as PV.
- Carbon taxes' impact on renewable energy projects has two sides. On one hand, they incentivise the deployment of RES by making them more economically convenient, but on the other hand they penalise the company, by increasing costs of fossil generation that can be lowered only up to a certain extent, thus reducing utilities' economic availability for new investments. In the case of Faial, it can be observed that the optimality front in the scenarios with carbon taxes features higher RES and BESS capacities than the one in the scenario without carbon tax, at parity of NPV, thus allowing for higher REF.
- Geothermal energy can cover a key role for the energy transition of the Azores, thanks to its constant production throughout the year. In the case of Faial, geothermal is the first technology

to enter in the optimal solutions, often even without any storage means in the system. For example, in the scenario with 6 €/ton carbon tax, a geothermal plant of around 4 MW of capacity can lift the REF in the system to 65%, which can become 75% with a 5.5 MW geothermal plant and 6.2 MWh of BESS, still allowing for a positive NPV.

Anyway, the feasibility of geothermal installations depends mainly on the success of the drilling phase and on the presence of an underground reservoir to facilitate heat exchange. As for the scaling of the costs with size, which allows larger plants to be more likely to be developed, the possibility of geothermal in Faial can become even more concrete if in future the grids of Faial, Pico and São Jorge are connected.

- Considering the increasing deployment of RES, new SR management strategies are needed to make islanded energy systems more flexible and better able to exploit the fluctuating renewable production. Old and rigid SR requirements force curtailment of the renewable energy production, and impose a limit to the possible RES penetration, which new technologies for storage and control systems allow to overcome. The most evident consequence is the fact that wind capacity only increases in the optimisation model when all other technologies are constrained, and when there is a high minimum REF constraint. Still, the wind penetration in the system is already high enough to force a large usage of spinning reserve, and therefore forcing curtailments amounting to 7% of the total yearly demand in the base case. Installing more renewables the curtailed energy increases, and becomes 53% of the total demand in the optimal design chosen for the sensitivity analysis.
- Fossil fuel generators still play an important role, and their usage can not be completely avoided especially in microgrids and isolated systems. In the case of Faial, their usage can be reduced in a technically and economically feasible way of more than 55% from the current situation, allowing to save more tham 365000 tons of $CO_2$ every year. However, it is unlikely that isolated energy systems will be able to operate for long periods in total absence of thermal generators in the near future, and at least for the next two decades. Still, the environmental impact derived from their necessity can be mitigated, by choosing blends with a share of biofuels in their composition, as far as technological constraints allow it.

Many other approaches and technologies, such as price-driven or centrally managed demand side management or Vehicle-to-Grid (V2G) energy storage, are very promising and will probably play an important role in the energy transition, especially in microgrids.

Renewable energy sources are not only the future of energy generation, but its present, and especially in a region rich of resources like the Azores archipelago RES can prove to be not only the best choice in terms of environmental friendliness, but also in terms of economical convenience.

# REFERENCES


[1] International Energy Agency, World Energy Outlook 2017, OECD/IEA, 2017.

[2] G. Notton, L. Stoyanov, M. Ezzat, V. Lararov, S. Diaf and C. Cristofari, "Integration Limit of Renewable Energy Systems in Small Electrical Grid," *Energy Procedia,* no. 6, pp. 651-665, 2011.

[3] EDA, "Plano estratégico plurianual e orçamento para 2018," 2017. [Online]. Available: http://www.eda.pt/Mediateca/Publicacoes/Paginas/PEPO.aspx.

[4] D. Schnitzer, D. S. Lounsbury, J. P. Carvallo, R. Deshmukh, J. Apt and D. M. Kammen, "Microgrids for Rural Electrification: A critical review of best practices based on seven case studies," United Nations Foundation, January 2014. [Online]. Available: https://rael.berkeley.edu/wp-content/uploads/2015/04/MicrogridsReportEDS.pdf.

[5] H. Borhanazad, S. Mekhilef, R. Saidur and G. Boroumandjazi, "Potential application of renewable energy for rural electrification in Malaysia," *Renewable Energy,* no. 59, pp. 210-219, 2013.

[6] T. S. Ustun, C. Ozansoy and A. Zayegh, "Recent developments in microgrids and example cases around the world - A review," *Renewable and Sustainable Energy Reviews 15,* p. 4030–4041, 2011.

[7] A. Gupta, R. P. Saini and M. P. Sharma, "Modelling of hybrid energy system - Part I: Problem formulation and model development," *Renewable Energy,* no. 36, pp. 459-465, 2011.

[8] A. Gupta, R. P. Saini and M. P. Sharma, "Modelling of hybrid energy system - Part II: Combined dispatch strategies and solution algorithm," *Renewable Energy,* no. 36, pp. 466-473, 2011.

[9] A. Gupta, R. P. Saini and M. P. Sharma, "Modelling of hybrid energy system - Part III: Case study with simulation results," *Renewable Energy,* no. 36, pp. 474-481, 2011.

[10] M. Bortolini, M. Gamberi, A. Graziani and F. Pilati, "Economic and environmental bi-objective design of an off-grid photovoltaic–battery–diesel generator hybrid energy system," *Energy Conversion and Management,* no. 106, pp. 1024-1038, 2015.

[11] G. Tina, S. Gagliano and S. Raiti, "Hybrid solar/wind power system probabilistic modelling for long-term performance assessment," *Solar Energy,* no. 80, pp. 578-588, 2006.

[12] C.-a. Li, R. B. Johnson and A. J. Svoboda, "A new unit commitment method," *IEEE Transactions on Power Systems,* vol. 12, no. 1, February 1997.

[13] T. Senjyu, T. Miyagi, S. A. Yousuf, N. Urasaki and T. Funabashi, "A technique for unit commitment with energy storage system," *Electrical Power and Energy Systems,* vol. 29, pp. 91-98, 2007.

[14] P. A. Ruiz, C. R. Philbrick, E. Zak, K. W. Cheung and P. W. Sauer, "Uncertainty Management in the Unit Commitment Problem," *IEEE Transactions on Power Systems,* vol. 24, no. 2, May 2009.

[15] A. Tuohy, P. Meibom, E. Denny and M. O'Malley, “Unit Commitment for systems with significant wind penetration,” *IEEE Transactions on Power Systems,* vol. 24, no. 2, pp. 592-601, May 2009.

[16] J. J. Hargreaves and B. F. Hobbs, “Commitment and dispatch with uncertain wind generation by dynamic programming,” *IEEE Transactions on Sustainable Energy,* vol. 3, no. 4, pp. 724-734, October 2012.

[17] B. Bahmani-Firouzi, E. Farjah and R. Azizipanah-Abarghooee, “An efficient scenario-based and fuzzy self-adaptive learning particle swarm optimization approach for dynamic economic emission dispatch considering load and wind power uncertainties,” *Energy,* no. 50, pp. 232-244, 2013.

[18] M. Sharafi and T. Y. ELMekkawy, “Multi-objective optimal design of hybrid renewable energy systems using PSO-simulation based approach,” *Renewable Energy,* no. 68, pp. 67-79, 2014.

[19] G. J. Osorio, J. M. Lujano-Rojas, J. C. O. Matias and J. P. S. Catalão, “A probabilistic approach to solve the economic dispatch problem with intermittent renewable energy sources,” *Energy 82,* pp. 949 - 959, 2015.

[20] J. M. Lujano-Rojas, G. J. Osorio and J. P. S. Catalão, “New probabilistic method for solving economic dispatch and unit commitment problems incorporating uncertainty due to renewable energy integration,” *Electrical Power and Energy Systems,* no. 78, pp. 61-71, 2016.

[21] S. M. Dawoud, L. Xiangning and M. I. Okba, “Hybrid renewable microgrid optimization techniques: A review,” *Renewable and Sustainable Energy Reviews,* no. 82, pp. 2039-2052, 2017.

[22] A. Setas Lopes, R. Castro and C. Silva, “Metaheuristic Methods Applied to the Pumps and Turbines Configuration Design of Water Pumped Storage Systems,” *Journal of Energy Storage,* no. 18, pp. 196-205, 2018.

[23] H. Branco, R. Castro and A. Setas Lopes, “Battery energy storage systems as a way to integrate renewable energy in small isolated power systems,” *Energy for Sustainable Development,* vol. 43, pp. 90-99, April 2017.

[24] I. Miranda, N. Silva and H. Leite, “A Holistic Approach to the Integration of Battery Energy Storage Systems in Island Electric Grids With High Wind Penetration,” *IEEE Transactions on Sustainable Energy, vol. 7, No. 2,* pp. 775-785, April 2016.

[25] D. Neves, A. Pina and C. A. Silva, “Assessment of the potential use of demande response in DHW systes on isolated microgrids,” *Renewable Energy,* vol. 115, pp. 989 - 998, 2018.

[26] F. Guzzi, D. Neves and C. A. Silva, “Integration of smart grid mechanisms on microgrids energy modelling,” vol. 129, pp. 321 - 330, April 2017.

[27] A. Pina, P. Baptista, C. Silva and P. Ferrão, “Energy reduction potential from the shift to electric vehicles: The Flores island case study,” *Energy Policy 67,* pp. 37 - 47, 2013.

[28] A. Setas Lopes, R. Castro and J. M. Ferreira de Jesus, “Contributions to the preliminary assessment of a Water Pumped Storage System in Terceira Island (Azores),” *Journal of Energy Storage,* no. 6, pp. 59-69, 2016.

[29] P. Stenzel, A. Schreiber, J. Marx, C. Wulf, M. Schreieder and L. Stephan, “Renewable energies for Graciosa Island, Azores - Life Cycle Assessment of electricity generation,” *Energy Procedia,* vol. 135, pp. 62 - 74, 2017.

[30] NREL, “Impacts of Solar Power on Operating Reserve Requirements,” December 2012. [Online]. Available: http://www.nrel.gov/docs/fy13osti/56596.pdf.

[31] The Wind Power, “Vestas V52/850,” 9 1 2018. [Online]. Available: https://www.thewindpower.net/turbine_en_27_vestas_v52-850.php. [Accessed 05 02 2018].

[32] V. Stanojevic, “Unit commitment by dynamic programming method,” 5 Jul 2011. [Online]. Available: https://www.mathworks.com/matlabcentral/fileexchange/32073-unit-commitment-by-dynamic-programming-method. [Accessed 19 June 2018].

[33] W. J. Hobbs, G. Hermon, S. Warner and G. B. Shelbe, “An enhanced dynamic programming approach for unit commitment,” *IEEE Transactions on Power Systems,* vol. 3, no. 3, pp. 1201-1205, 1988.

[34] EDA, “CARE 2016 - Caracterizaçao das redes de transporte e distribução de energia eléctrica da Região Autonoma dos Açores,” 2017. [Online]. Available: http://www.eda.pt/Regulacao/Lists/CaracterizacaodeRedes1/Attachments/27/CARE%202016.pdf.

[35] ERSE Entitade Reguladora dos Serviços Energeticos, “Caracterização da procura de energia elétrica em 2017,” 2016. [Online]. Available: http://www.erse.pt/pt/electricidade/tarifaseprecos/2017/Documents/Caracteriza%C3%A7%C3%A3o%20Procura%20EE%202017%20(Final).pdf.

[36] Região Autónoma dos Açores - Presidência do Governo, “Estratégia Regional para as Alterações Climáticas,” 19 10 2011. [Online]. Available: http://servicos-sraa.azores.gov.pt/grastore/SRAM/Resolu%C3%A7ao%20-%20estrat%C3%A9gia%20para%20as%20altera%C3%A7%C3%B5es%20clim%C3%A1ticas.pdf.

[37] INE/PORDATA, “População residente, estimativas a 31 de Dezembro 2016,” 25 01 2018. [Online]. Available: https://www.pordata.pt/Municipios/Popula%C3%A7%C3%A3o+residente++estimativas+a+31+de+Dezembro-120.

[38] EDA, “Produçao e Consumo - Dezembro 2017,” January 2018. [Online]. Available: http://www.eda.pt/Mediateca/Publicacoes/Producao/_layouts/15/WopiFrame.aspx?sourcedoc={1611f66e-9758-4666-972d-165d12c2b498}&action=view. [Accessed 14 03 2018].

[39] EDA, “Rotulagem de Energia Elétrica 2017,” 2018. [Online]. Available: http://www.eda.pt/Regulacao/Rotulagem/Paginas/Resultados.aspx. [Accessed 23 02 2018].

[40] EDP, “Origens da Eletricidade,” 2018. [Online]. Available: http://www.edpsu.pt/pt/origemdaenergia/Pages/OrigensdaEnergia.aspx. [Accessed 23 02 2018].

[41] EDA, “Relatorio e Contas 2016,” 2017. [Online]. Available: http://www.eda.pt/Investidores/Lists/Relatorios/Attachments/23/RC%20EDA%202016.pdf.

[42] ABB, “Case study - Faial Island wind/diesel/RMC 600,” 2013. [Online]. Available: https://library.e.abb.com/public/506484bf21544754bd8ac6d557b7b2f0/Faial_Island_Case_Study_EN.pdf .

[43] RTP Açores, “EDA vai desmantelar o parque eólico da Lomba dos Frades,” 13 09 2010. [Online]. Available: http://www.rtp.pt/acores/sociedade/eda-vai-desmantelar-o-parque-eolico-da-lomba-dos-frades-video_17155. [Accessed 03 02 2018].

[44] B2B Energias Renováveis, “EDA desmantela Parque eólico do Faial,” 15 September 2010. [Online]. Available: http://www.renewablesb2b.com/ahk_portugal/pt/portal/windpower/news/show/9dcc3b0083940b88/eda-desmantela-parque-eolico-do-faial. [Accessed 3 2 2018].

[45] RTP Açores, “Faial: EDA vai instalar novo parque de aerogeradores no Salão,” 4 4 2011. [Online]. Available: http://www.rtp.pt/acores/local/faial-eda-vai-instalar-novo-parque-de-aerogeradores-no-salao_20539. [Accessed 3 2 2018].

[46] INEGI, E2P, “Power plants list (R.A. Açores),” 2018. [Online]. Available: http://e2p.inegi.up.pt/index.asp.

[47] LG Electronics, “LG NeON 2 335W | 330W | 325W,” 23 May 2017. [Online]. Available: http://www.lg-solar.com/downloads/spec-sheet/DS_NeON2_60cells.pdf. [Accessed 20 06 2018].

[48] MINES ParisTech / Transvalor, “Helioclim-1,” 2018. [Online]. Available: http://www.soda-pro.com/web-services/radiation/helioclim-1. [Accessed 02 05 2018].

[49] T. Cebecauer and M. Suri, “Typical Meteorological Year data: SolarGIS approach,” *Energy Procedia 69,* p. 1958 – 1969, 2015.

[50] T. Huld, E. Paietta, P. Zangheri and I. Pinedo Pascua, “Assembling Typical Meteorological Year Data Sets for Building Energy Performance Using Reanalysis and Satellite-Based Data,” *Atmosphere,* 2018.

[51] S. Conti, T. Crimi, S. Raiti, G. Tina and U. Vagliasindi, “Probabilistic approach to assess the performance of grid-connected PV systems,” *Proceedings of 7th International Conference on Probabilistic Methods applied to Power Systems,* 2002.

[52] J. Bright, . C. Smith, P. Taylor and R. Crook, “Stochastic generation of synthetic minutely irradiance time series derived from mean hourly weather observation data,” *Solar Energy,* no. 115, pp. 229-242, 2015.

[53] Climate-Data.org, “Clima: Faial,” 21 05 2018. [Online]. Available: https://it.climate-data.org/location/720523/.

[54] J. A. Duffie and W. A. Beckman, Solar Engineering of Thermal Processes, 4th ed., Wiley, 2013.

[55] D. C. Jordan, T. J. Silverman, B. Sekulic and S. R. Kurtz, “PV degradation curves: non-linearities and failure modes,” *Progress in Photovoltaics: Research and Applications,* no. 25, pp. 583-591, 2017.

[56] D. C. Jordan and S. R. Kurtz, “Photovoltaic Degradation Rates - An Analytical Review,” *Progress in Photovoltaics: Research and Applications,* June 2012.

[57] Governo dos Açores, “Inaugurada Central Geotérmica da Terceira,” 20 November 2017. [Online]. Available: http://www.azores.gov.pt/Gra/sreat-dre/conteudos/noticias/2017/Novembro/inauguracao-geotermica-terceira.htm. [Accessed 9 September 2018].

[58] Tesla, “PowerPack,” 2018. [Online]. Available: https://www.tesla.com/it_IT/powerpack?redirect=no. [Accessed 4 July 2018].

[59] Electrek, “Tesla Model 3 battery packs have capacities of ~50 kWh and ~75 kWh, says Elon Musk,” 8 August 2017. [Online]. Available: https://electrek.co/2017/08/08/tesla-model-3-battery-packs-50-kwh-75-kwh-elon-musk/. [Accessed 3 September 2018].

[60] Autonomous Region of the Azores, “Assumptions and context for the Action Plan 2014-2020,” 2013.

[61] INE, “Sales of new vehicles per 1000 inhabitants (No.) by Place of residence (NUTS - 2013) and Type of vehicle; Annual,” 21 November 2017. [Online]. Available: https://www.ine.pt/xportal/xmain?xpid=INE&xpgid=ine_indicadores&indOcorrCod=0008464&contexto=bd&selTab=tab2. [Accessed 5 September 2018].

[62] Caterpillar/MaK, “M32C - Long-Stroke Diesel Engines for Maximum Efficiency and High Reliability,” 2014. [Online].

[63] IEA, “CO2 emissions from fuel combustion: beyond 2020 documentation,” 2012.

[64] INE, PORDATA, “Inflation Rate (Growth Rate - Consumer Price Index): total and individual consumption by purpose,” 2018. [Online]. Available: https://www.pordata.pt/en/Portugal/Inflation+Rate+(Growth+Rate+++Consumer+Price+Index)+total+and+individual+consumption+by+purpose-2315. [Accessed 26 June 2018].

[65] B. Valpy, P. English, A. Martinez and E. Simonot, “Future renewable energy costs: onshore wind,” BVG Associates, KIC InnoEnergy, 2014.

[66] IRENA, “Renewable Power Generation Costs in 2017,” 2018. [Online]. Available: https://www.irena.org/-/media/Files/IRENA/Agency/Publication/2018/Jan/IRENA_2017_Power_Costs_2018.pdf.

[67] Andy Walker, NREL, “PV O&M Cost Model and Cost Reduction,” 28 February 2017. [Online]. Available: https://www.nrel.gov/docs/fy17osti/68023.pdf.

[68] H. Kristjánsdóttir and Á. Margeirsson, “Geothermal Cost and Investment Factors,” in *Comprehensive Renewable Energy*, vol. 7, Elsevier, 2012, pp. 261-272.

[69] Electrek, “Tesla slashes price of the Powerpack system by another 10% with new generation,” 14 November 2016. [Online]. Available: https://electrek.co/2016/11/14/tesla-powerpack-2-price/.

[70] Lazard, “Lazard's Levelized Cost of Storage - Version 3.0,” 2017. [Online]. Available: https://www.lazard.com/media/450338/lazard-levelized-cost-of-storage-version-30.pdf.

[71] Fraunhofer (ISE), “Current and Future Cost of Photovoltaics. Long-term scenarios for Market Development, System Prices and LCOE of Utility-Scale PV Systems. Study on behalf of Agora Energiewende,” 2015. [Online]. Available: https://www.ise.fraunhofer.de/content/dam/ise/de/documents/publications/studies/AgoraEnergiewende_Current_and_Future_Cost_of_PV_Feb2015_web.pdf.

[72] European Commission, “Energy Union Factsheet Portugal,” 2017. [Online]. Available: https://ec.europa.eu/commission/sites/beta-political/files/energy-union-factsheet-portugal_en.pdf.

[73] Climatemps, “Rainfall/ Precipitation in Horta, Faial, Azores,” 2017. [Online]. Available: http://www.horta.climatemps.com/precipitation.php. [Accessed 18 August 2018].

# ANNEX A – OPTIMISATION RESULTS IN DETAIL

**TABLE 11 – OPTIMISATION RESULTS IN DETAIL, WITH NPV MAXIMISED IN COMPARISON WITH RESPECTIVE BASE CASE**

| | | REF | wind kW | PV kW | geo kW | storage kWh | NPVcomp M€ |
|---|---|---|---|---|---|---|---|
| WITH GEOTHERMAL | No carbon tax | 40,0% | 4250 | 0,0 | 1312,0 | 0,0 | -3,243 |
| | | 45,0% | 4250 | 0,0 | 1781,8 | 0,0 | -4,553 |
| | | 50,0% | 4250 | 0,0 | 2270,5 | 0,0 | -5,986 |
| | | 55,0% | 4250 | 0,0 | 2783,8 | 0,0 | -7,581 |
| | | 60,0% | 4250 | 0,0 | 3340,2 | 0,0 | -9,455 |
| | | 65,0% | 4250 | 0,0 | 3999,1 | 86,3 | -11,892 |
| | | 70,0% | 4250 | 0,0 | 4677,4 | 897,8 | -14,391 |
| | | 75,0% | 4250 | 0,0 | 5503,7 | 6208,8 | -22,230 |
| | | 80,0% | 4250 | 1493,8 | 4641,8 | 4179746,0 | -5074,362 |
| | | 85,0% | 4250 | 0,0 | 5204,6 | 9117354,1 | -11053,021 |
| | Carbon tax 6 €/ton$_{CO2}$ | **REF** | **wind kW** | **PV kW** | **geo kW** | **storage kWh** | **NPV M€** |
| | | 65,2% | 4250 | 0 | 4066,7 | 0 | 9,811 |
| | | 65,2% | 4250 | 0 | 4066,7 | 0,0 | 9,811 |
| | | 65,2% | 4250 | 0 | 4066,7 | 0,0 | 9,811 |
| | | 70,0% | 4250 | 0 | 4909,7 | 197,1 | 8,969 |
| | | 75,0% | 4250 | 0 | 5503,9 | 6207,8 | 0,043 |
| | | 80,0% | 4250 | 32910,7 | 4872,5 | 3817,0 | -24,962 |
| | Carbon tax 12 €/ton$_{CO2}$ | **REF** | **wind kW** | **PV kW** | **geo kW** | **storage kWh** | **NPV M€** |
| | | 68,4% | 4250 | 0,0 | 4640,8 | 0,0 | 31,032 |
| | | 68,4% | 4250 | 0,0 | 4640,8 | 0,0 | 31,032 |
| | | 70,0% | 4250 | 0,0 | 4989,2 | 25,8 | 30,761 |
| | | 75,0% | 4250 | 2415,0 | 7500,0 | 0,0 | 15,306 |
| | | 80,0% | 4250 | 32605,1 | 4890,8 | 3952,4 | -2,754 |
| | | 85,0% | 4250 | 57372,8 | 4813,9 | 3561,3 | -20,612 |
| WITHOUT GEOTHERMAL | No carbon tax | **REF** | **wind kW** | **PV kW** | **geo kW** | **storage kWh** | **NPV M€** |
| | | 24,8% | 4250 | 0,0 | 0,0 | 0,0 | 0,000 |
| | | 25,0% | 4250 | 22,5 | 0,0 | 112,0 | -0,199 |
| | | 30,0% | 4250 | 2549,8 | 0,0 | 0,0 | -3,547 |
| | | 35,0% | 4250 | 5410,0 | 0,0 | 0,0 | -5,665 |
| | | 40,0% | 4250 | 9547,9 | 0,0 | 0,0 | -8,832 |
| | | 45,0% | 4250 | 15515,6 | 0,0 | 1183,8 | -15,341 |
| | | 50,0% | 4250 | 20923,1 | 0,0 | 5268,0 | -22,346 |
| | | 55,0% | 4250 | 27092,1 | 0,0 | 10621,2 | -31,306 |
| | | 60,0% | 4250 | 32319,1 | 0,0 | 18004,9 | -43,165 |
| | | 65,0% | 4250 | 43347,4 | 0,0 | 22596,2 | -56,288 |
| | | 70,0% | 4250 | 59205,1 | 0,0 | 24810,2 | -70,127 |
| | | 75,0% | 4250 | 73284,4 | 0,0 | 28946,1 | -84,615 |
| | | 80,0% | 4250 | 92294,6 | 0,0 | 30518,8 | -99,558 |
| | | 85,0% | 4250 | 117185,0 | 0,0 | 28854,2 | -114,718 |
| | Carbon tax 6 €/ton$_{CO2}$ | **REF** | **wind kW** | **PV kW** | **geo kW** | **storage kWh** | **NPV M€** |
| | | 35,9% | 4250 | 6016,5 | 0 | 0,0 | -0,615 |
| | | 40,0% | 4250 | 9547,9 | 0 | 0,0 | -0,897 |
| | | 45,0% | 4250 | 14824,6 | 0 | 1700,7 | -3,413 |
| | | 50,0% | 4250 | 20692,7 | 0 | 5444,8 | -9,912 |
| | | 55,0% | 4250 | 26031,7 | 0 | 11389,0 | -18,361 |
| | | 60,0% | 4250 | 31855,5 | 0 | 18350,3 | -28,375 |
| | | 65,0% | 4250 | 38110,6 | 0 | 26231,5 | -39,836 |
| | | 70,0% | 4250 | 49948,3 | 0 | 31123,8 | -52,642 |
| | | 75,0% | 4250 | 67797,7 | 0 | 32599,7 | -66,386 |
| | Carbon tax 12 €/ton$_{CO2}$ | **REF** | **wind kW** | **PV kW** | **geo kW** | **storage kWh** | **NPV M€** |
| | | 40,2% | 4250 | 9755,2 | 0,0 | 0,0 | 7,568 |
| | | 45,0% | 4250 | 14792,3 | 0,0 | 1725,8 | 5,892 |
| | | 50,0% | 4250 | 20269,6 | 0,0 | 5776,0 | 1,194 |
| | | 55,0% | 4250 | 25012,5 | 0,0 | 12222,0 | -5,355 |
| | | 60,0% | 4250 | 30340,4 | 0,0 | 19550,0 | -13,465 |
| | | 65,0% | 4250 | 36282,1 | 0,0 | 27660,1 | -23,150 |
| | | 70,0% | 4250 | 46848,3 | 0,0 | 33498,9 | -34,661 |
| | | 75,0% | 4250 | 63484,6 | 0,0 | 35880,0 | -47,780 |
| | | 80,0% | 4250 | 80260,7 | 0,0 | 39063,6 | -61,814 |

TABLE 12 – OPTIMISATION RESULTS WITH 1.5 MW LIMITATION ON PV

| | | REF | wind kW | PV kW | geo kW | storage kWh | NPVcomp M€ |
|---|---|---|---|---|---|---|---|
| WITH GEOTHERMAL | No carbon tax | 40,0% | 4250 | 0,0 | 1312,0 | 0,0 | -3,243 |
| | | 45,0% | 4250 | 0,0 | 1781,8 | 0,0 | -4,553 |
| | | 50,0% | 4250 | 0,0 | 2270,5 | 0,0 | -5,986 |
| | | 55,0% | 4250 | 0,0 | 2783,8 | 0,0 | -7,581 |
| | | 60,0% | 4250 | 0,0 | 3340,2 | 0,0 | -9,455 |
| | | 65,0% | 4250 | 0,0 | 3999,1 | 86,3 | -11,892 |
| | | 70,0% | 4250 | 0,0 | 4677,4 | 897,8 | -14,391 |
| | | 75,0% | 4250 | 0,0 | 5503,7 | 6208,8 | -22,230 |
| | | 80,0% | 4250 | 1493,8 | 4641,8 | 4179746,0 | -5074,362 |
| | | 85,0% | 4250 | 0,0 | 5204,6 | 9117354,1 | -11053,021 |
| | Carbon tax 6 €/ton$_{CO2}$ | **REF** | **wind kW** | **PV kW** | **geo kW** | **storage kWh** | **NPVcomp M€** |
| | | 65,2% | 4250 | 0,0 | 4066,7 | 0,0 | 9,811 |
| | | 75,0% | 4250 | 0,0 | 5503,9 | 6207,8 | 0,043 |
| | | 80,0% | 4250 | 1500,0 | 7500,0 | 4977278,4 | -6032,635 |
| | | 85,0% | 4250 | 0,0 | 5194,9 | 9116816,1 | -11029,995 |
| | | 90,0% | 4250 | 1500,0 | 7500,0 | 14808048,1 | -17936,384 |
| | | 95,0% | 4250 | 0,0 | 5254,4 | 19043204,0 | -23049,835 |
| | | 100,0% | 4250 | 1500,0 | 7500,0 | 24460392,8 | -29624,083 |
| | Carbon tax 12 €/ton$_{CO2}$ | **REF** | **wind kW** | **PV kW** | **geo kW** | **storage kWh** | **NPVcomp** |
| | | 68,4% | 4250 | 0 | 4640,8 | 0,0 | 31,032 |
| | | 68,4% | 4250 | 0 | 4640,8 | 0,0 | 31,032 |
| | | 70,0% | 4250 | 0 | 4989,2 | 25,8 | 30,761 |
| | | 75,0% | 4250 | 1500 | 7500 | 186131,3 | -208,873 |
| | | 80,0% | 4250 | 1500 | 7500 | 4977278,4 | -6010,312 |
| | | 85,0% | 4250 | 1500 | 7500 | 9989384,9 | -12079,303 |
| WITHOUT GEOTHERMAL | No carbon tax | **REF** | **wind kW** | **PV kW** | **geo kW** | **storage kWh** | **NPVcomp** |
| | | 24,8% | 4250,0 | 0 | 0 | 0,0 | 0,000 |
| | | 24,8% | 4250,0 | 0 | 0 | 0,0 | 0,000 |
| | | 30,0% | 4250,0 | 1500 | 0 | 6166,9 | -10,729 |
| | | 35,0% | 4590,8 | 1500 | 0 | 52161,4 | -63,840 |
| | | 40,0% | 5250,6 | 1500 | 0 | 207719,0 | -252,238 |
| | Carbon tax 6 €/ton$_{CO2}$ | **REF** | **wind kW** | **PV kW** | **geo kW** | **storage kWh** | **NPVcomp** |
| | | 24,8% | 4250 | 0 | 0 | 0,0 | 0,000 |
| | | 24,8% | 4250 | 0 | 0 | 0,0 | 0,000 |
| | | 25,0% | 4250 | 29,4 | 0 | 93,9 | -0,124 |
| | | 30,0% | 4250 | 1500 | 0 | 6166,9 | -6,708 |
| | | 35,0% | 4564,882 | 1500 | 0 | 52219,9 | -58,904 |
| | | 40,0% | 5250,572 | 1500 | 0 | 207726,6 | -245,196 |
| | Carbon tax 12 €/ton$_{CO2}$ | **REF** | **wind kW** | **PV kW** | **geo kW** | **storage kWh** | **NPVcomp** |
| | | 28,0% | 4250,0 | 1500 | 0 | 0,0 | -15,591 |
| | | 30,0% | 4250,0 | 1500 | 0 | 6166,9 | -20,379 |
| | | 35,0% | 4564,9 | 1500 | 0 | 52218,8 | -70,616 |
| | | 40,0% | 5250,6 | 1500 | 0 | 207718,6 | -254,793 |
| | | 45,0% | 6311,6 | 1500 | 0 | 568237,9 | -688,534 |
| | | 50,0% | 6329,9 | 1500 | 0 | 1878800,8 | -2270,818 |
| | | 55,0% | 8007,6 | 1500 | 0 | 5258634,3 | -6368,019 |